On Courant's nodal domain property for linear combinations of eigenfunctions

Pierre Bérard, Bernard Helffer

ON COURANT'S NODAL DOMAIN PROPERTY FOR LINEAR COMBINATIONS OF EIGENFUNCTIONS

PIERRE BÉRARD AND BERNARD HELFFER

Abstract. We revisit Courant's nodal domain property for linear combinations of eigenfunctions, and propose new, simple and explicit counterexamples for domains in $\mathbb{R}^2$, $\mathbb{S}^2$, $\mathbb{T}^2$, and $\mathbb{R}^3$, including convex domains.

1. Introduction

Let $\Omega \subset \mathbb{R}^d$ be a bounded open domain or, more generally, a compact Riemannian manifold with boundary.

Consider the eigenvalue problem

$$\begin{cases} -\Delta u &= \lambda\, u \quad \text{in } \Omega\,, \\ B(u) &= 0 \qquad \text{on } \partial\Omega\,, \end{cases} \tag{1.1}$$

where $B(u)$ is some homogeneous boundary condition on $\partial\Omega$, so that we have a self-adjoint boundary value problem (including the empty condition if Ω is a closed manifold). For example, we can choose $D(u) = u|_{\partial\Omega}$ for the Dirichlet boundary condition, or $N(u) = \frac{\partial u}{\partial \nu}|_{\partial\Omega}$ for the Neumann boundary condition.

Call $H(\Omega, B)$ the associated self-adjoint extension of $-\Delta$, and list its eigenvalues in nondecreasing order, counting multiplicities,

$$0 \le \lambda_1(\Omega, B) < \lambda_2(\Omega, B) \le \lambda_3(\Omega, B) \le \cdots \tag{1.2}$$

For any $n \ge 1$, define the number

$$\tau(\Omega, B, n) = \min\{k \mid \lambda_k(\Omega, B) = \lambda_n(\Omega, B)\}. \tag{1.3}$$

Shorthand. We use $u \in \lambda_n(\Omega, B)$ as a shorthand for u is an eigenfunction of $H(\Omega, B)$ associated with the eigenvalue $\lambda_n(\Omega, B)$ i.e.,

$$H(\Omega, B)(u) = \lambda_n(\Omega, B)\, u\,.$$

Given a real continuous function v on Ω, define its *nodal set*

$$\mathcal{Z}(v) = \overline{\{x \in \Omega \mid v(x) = 0\}}\,, \tag{1.4}$$

Date: August 27, 2017.

2010 *Mathematics Subject Classification.* 35P99, 35Q99, 58J50.

Key words and phrases. Eigenfunction, Nodal domain, Courant nodal domain theorem.

and call $\beta_0(v)$ the number of connected components of $\Omega \setminus \mathcal{Z}(v)$ i.e., the number of *nodal domains* of v.

Theorem 1.1. *[Courant (1923)]*
For any nonzero $u \in \lambda_n(\Omega, B)$,

$$\beta_0(u) \leq \tau(\Omega, B, n) \leq n\,. \tag{1.5}$$

Courant's nodal domain theorem can be found in [10, Chap. V.6]. A footnote in [10, p. 454] (see also the second footnote in [9, p. 394]) indicates that this theorem also holds for any linear combination of the n first eigenfunctions, and refers to the PhD thesis of Horst Herrmann (Göttingen, 1932) [17].

For later reference, we write a precise statement. Given $r > 0$, denote by $\mathcal{L}(\Omega, B, r)$ the space of linear combinations of eigenfunctions of $H(\Omega, B)$ associated with eigenvalues less than or equal to r,

$$\mathcal{L}(\Omega, B, r) = \left\{ \sum_{\lambda_j(\Omega,B)\leq r} c_j\, u_j \mid c_j \in \mathbb{R}, u_j \in \lambda_j(\Omega, B) \right\}. \tag{1.6}$$

Statement 1.2. *[Extended Courant Property]*
Let $v \in \mathcal{L}\,(\Omega, B, \lambda_n(\Omega, B))$ be any linear combination of eigenfunctions associated with the n first eigenvalues of the eigenvalue problem (1.1). Then,

$$\beta_0(v) \leq \tau(\Omega, B, n) \leq n\,. \tag{1.7}$$

The footnote in [10, p. 454] claims that Statement 1.2 is true.

Remarks on the Extended Courant Property.
1. Statement 1.2 is true for Sturm-Liouville equations. This was first announced by C. Sturm in 1833, [27] and proved in [28]. Other proofs were later on given by J. Liouville and Lord Rayleigh who both cite Sturm explicitly, see [7] for more details.
2. Å. Pleijel mentions Statement 1.2 in his well-known paper [26] on the asymptotic behaviour of the number of nodal domains of a Dirichlet eigenfunction associated with the n-th eigenvalue for a plane domain. At the end of the paper, he also considers the Neumann boundary condition.
"In order to treat, for instance the case of the free three-dimensional membrane $[0, \pi]^3$, it would be necessary to use, in a special case, the theorem quoted in [9], p. 394[1]. This theorem which generalizes part of the Liouville-Rayleigh theorem for the string asserts that a linear combination, with constant coefficients, of the n first eigenfunctions can have at most n nodal domains. However, as far as I have been able to find there is no proof of this assertion in the literature."

[1]Pleijel refers to the German edition, this is p. 454 in the English edition [10].

3. Arnold [2], see also [20, 21] and [19], mentions that he actually discussed the footnote in [10, p. 454] with R. Courant, that the *Extended Courant Property* cannot be true in general, and that O. Viro produced counterexamples for the sphere. More precisely, as early as 1973, V. Arnold [1] pointed out that, when Ω is the round sphere $\mathbb{S}^N$, the *Extended Courant Property* is related to Hilbert's 16th problem. Indeed, the eigenfunctions of the Laplace-Beltrami operator on $\mathbb{S}^N$ are the spherical harmonics i.e., the restrictions to the sphere of the harmonic homogeneous polynomials, so that the linear combinations of spherical harmonics of degree less than or equal to n are the restrictions to the sphere of the homogeneous polynomials of degree n in $(N+1)$ variables. The following citation is taken from [3].
Eigen oscillations of the sphere with the standard metric are described by spherical functions, i.e., polynomials. Therefore the Courant statement cited above implies the following estimate

$$\dim_{\mathbb{R}} H_0(\mathbb{R}P^N - V_n, \mathbb{R}) \leq C^N_{N+n-2} + 1 \qquad (1)$$

for the number of connected components of the complement to an algebraic hypersurface of degree n in the N-dimensional projective space.

For planar curves ($N = 2$), the estimation (1) *is exact (it turns into equality on a configuration of n lines in general position) and can be proven independently of the Courant statement. For smooth surfaces of degree* 4 *in $\mathbb{R}P^3$ the estimation is also exact and proved (by V.M. Kharlamov).*

In the general case, the Courant statement is false (a counterexample can be constructed by a small perturbation of the standard metric on the sphere). Nonetheless the estimation (1) *seems to be plausible: for proving it one has to verify the Courant statement only for oscillation of the sphere (or the projective space) with the standard metric.*[1]

[1] *Translator's remark: the inequality* (1) *does not hold true for surfaces of even degree ≥ 6 in $\mathbb{R}P^3$. Counterexamples to* (1) *were constructed in the paper of O. Viro, "Construction of multicomponent real algebraic surfaces", Soviet Math. Dokl.* ***20****, N°. 5, 991–995 (1979).*

4. In [13], Gladwell and Zhu refer to Statement 1.2 as the *Courant-Herrmann conjecture*. They claim that this extension of Courant's theorem is not stated, let alone proved, in Herrmann's thesis or subsequent publications[2]. They consider the case in which Ω is a rectangle in $\mathbb{R}^2$, stating that they were not able to find a counterexample to the *Extended Courant Property* in this case. They also provide numerical evidence that there are counterexamples for more complicated (non convex) domains.

[2]The only relevant one seems to be [18].

The purpose of the present paper is to provide simple counterexamples to the *Extended Courant Property* for domains in $\mathbb{R}^2$, $\mathbb{T}^2$, $\mathbb{S}^2$, and $\mathbb{R}^3$, including convex domains.

The paper is organized as follows. In Section 2, we recall the ideas from [13]. In Sections 3, 4 and 5, we construct counterexamples by introducing cracks (with Neumann boundary condition), respectively on the rectangle, the rectangular torus, and the round sphere. In Section 6, we consider the cube with Dirichlet boundary condition. In Sections 7 and 8, we consider the equilateral triangle and the regular hexagon respectively, with either Dirichlet or Neumann boundary conditions. Section 10 contains numerical simulations kindly provided by V. Bonnaillie-Noël. In AppendixA, we give a summary of the description of the eigenvalues and eigenfunctions of the equilateral triangle with either Dirichlet or Neumann boundary conditions.

We point out that some of our examples rely on numerical computations of eigenvalues or nodal patterns of eigenfunctions.

Acknowledgements. The authors are very much indebted to Virginie Bonnaillie-Noël who performed the simulations and produced the pictures for Section 10.

2. Rectangular membrane, Dirichlet boundary condition

We summarize the ideas from [13].

Consider the square $\mathcal{S}_\pi =]0,\pi[^2$, with Dirichlet boundary condition. The eigenvalues are given by the numbers

$$q_2(m,n) = m^2 + n^2\,, \quad \text{for } m,n \in \mathbb{N}^\bullet\,.$$

More precisely, the Dirichlet eigenvalues of the square $\mathcal{S}_\pi$ are

$$\delta_1\ [2] < \delta_2 = \delta_3\ [5] < \delta_4\ [8] < \delta_5 = \delta_6\ [10] < \dots$$
$$< \delta_7 = \delta_8\ [13] < \delta_9 = \delta_{10}\ [17] < \delta_{11}\ [18] < \cdots$$

In this list the numbers in brackets are the actual values of the eigenvalues, for example, $\delta_2 = \delta_3 = 5$.

A corresponding complete family of Dirichlet eigenfunctions for the square $\mathcal{S}_\pi$ is given by the functions $\phi_{m,n}(x,y) = \sin(mx)\,\sin(ny)$ for $m,n \in \mathbb{N}^\bullet$. Using the classical Chebyshev polynomials, we have

$$\phi_{m,n}(x,y) = \phi_{1,1}(x,y)\,U_{m-1}(\cos x)\,U_{n-1}(\cos y)\,.$$

Given some positive r, denote by $\mathcal{L}_r$ the set $\mathcal{L}(\mathcal{S}_\pi, D, r)$. A function $\Phi \in \mathcal{L}_r$ is of the form

$$\Phi(x,y) := \sum_{q_2(m,n)\le r} c_{m,n}\,\phi_{m,n}(x,y)\,.$$

When looking at the nodal pattern of Φ, we can factor out the non-vanishing factor $\phi_{1,1}$, and consider instead the nodal pattern of the function,

$$\Phi_1(x,y) = \sum_{q_2(m,n)\leq r} c_{m,n}\, U_{m-1}(\cos x)\, U_{n-1}(\cos y)\,.$$

On the other-hand, using the diffeomorphism

$$F :]0,\pi[\ni (x,y) \mapsto (X,Y) := (\cos x, \cos y) \in]-1,1[\,,$$

we see that the nodal pattern of Φ_1 is diffeomorphic to the nodal pattern of the function,

$$\Psi(X,Y) := \sum_{q_2(m,n)\leq r} c_{m,n}\, U_{m-1}(X)\, U_{n-1}(Y)\,,$$

for $(X,Y) \in]-1,1[^2$.

Choosing $r = \delta_6 = 10$, i.e. linear combinations involving the six first Dirichlet eigenfunctions of the square, the linear combinations Ψ generate the subspace of $\mathbb{R}[X,Y]$ spanned by the family

$$\{1, X, Y, X^2, XY, Y^2\}$$

i.e., the polynomials in two variables, of degree less than or equal to 2. An immediate consequence of this analysis is that any $d \in \{1,2,3,4,5\}$ is achieved as $\beta_0(\Phi)$ for some $\Phi \in \mathcal{L}_{10}$. Notice that 5 is precisely Courant's bound $\tau(\mathcal{S}_\pi, D, 6)$, see Figure 2.1.

Choosing $r = \delta_{10} = 17$, i.e. linear combinations involving the ten first eigenvalues, the linear combinations generate the subspace spanned by the family

$$\{1, X, Y, X^2, XY, Y^2, XY^2, X^2Y, X^3, Y^3\}\,,$$

which corresponds to the polynomials of degree less than or equal to 3. An immediate consequence is that any $d \in \{1,2,3,4,5,6,7,8\}$ is achieved as $\beta_0(\Phi)$ for some $\Phi \in \mathcal{L}_{17}$. Notice that $8 < 9 = \tau(\mathcal{S}_\pi, D, 10)$.

Gladwell and Zhu conclude that it does not seem possible to find an example of $\Phi \in \mathcal{L}_{17}$ with nine or more nodal domains.

Table 1 CHC is true for the first 13 eigenfunctions on the square.

	m, n	New High Order Terms		Maximum No. of Nodal domains	
1	1, 1	1		1	
2, 3	1, 2 2, 1	X	Y	2	
4	2, 2	XY		4	
5, 6	1, 3 3, 1	X^2	Y^2	5	
7, 8	2, 3 3, 2	X^2Y	XY^2	7	
9, 10	1, 4 4, 1	X^3	Y^3	8	
11	3, 3	X^2Y^2		10	
12, 13	2, 4 4, 2	X^3Y	XY^3	12	

FIGURE 2.1. The pictures and computations of Gladwell-Zhu [13]

3. Rectangle with a crack

Let $\mathcal{R}$ be the rectangle $]0, 4\pi[\times]0, 2\pi[$. For $0 < a \leq 1$, let $C_a :=]0, a] \times \{\pi\}$ and $\mathcal{R}_a := \mathcal{R} \setminus C_a$. In this section, we only consider the Neumann boundary condition on C_a, and either the Dirichlet or Neumann boundary condition on $\partial\mathcal{R}$. The setting is the one described in [12, Section 8].

We call

$$\begin{cases} 0 < \delta_1(0) < \delta_2(0) \leq \delta_3(0) \leq \cdots \\ \text{resp.} \\ 0 = \nu_1(0) < \nu_2(0) \leq \nu_3(0) \leq \cdots \end{cases} \tag{3.1}$$

the eigenvalues of $-\Delta$ in $\mathcal{R}$, with Dirichlet (resp. Neumann) boundary condition on $\partial\mathcal{R}$. They are given by the numbers $\frac{m^2}{16} + \frac{n^2}{4}$, for pairs (m, n) of positive integers for the Dirichlet problem (resp. for pairs of non-negative integers for the Neumann problem). Corresponding eigenfunctions are products of sines (Dirichlet) or cosines (Neumann). The eigenvalues are arranged in non-decreasing order, counting multiplicities.

Similarly, call

$$\begin{cases} 0 < \delta_1(a) < \delta_2(a) \leq \delta_3(a) \leq \cdots \\ \text{resp.} \\ 0 = \nu_1(a) < \nu_2(a) \leq \nu_3(a) \leq \cdots \end{cases} \tag{3.2}$$

the eigenvalues of $-\Delta$ in $\mathcal{R}_a$, with Dirichlet (resp. Neumann) boundary condition on $\partial\mathcal{R}$, and Neumann boundary condition on C_a.

The first three Dirichlet (resp. Neumann) eigenvalues for the rectangle $\mathcal{R}$ are as follows.

(3.3)

Eigenvalue	Value	Pairs	Eigenfunctions
$\delta_1(0)$	$\frac{5}{16}$	$(1,1)$	$\phi_1(x,y) = \sin(\frac{x}{4})\,\sin(\frac{y}{2})$
$\delta_2(0)$	$\frac{1}{2}$	$(2,1)$	$\phi_2(x,y) = \sin(\frac{x}{2})\,\sin(\frac{y}{2})$
$\delta_3(0)$	$\frac{13}{16}$	$(3,1)$	$\phi_3(x,y) = \sin(\frac{3x}{4})\,\sin(\frac{y}{2})$
$\nu_1(0)$	0	$(0,0)$	$\psi_1(x,y) = 1$
$\nu_2(0)$	$\frac{1}{16}$	$(1,0)$	$\psi_2(x,y) = \cos(\frac{x}{4})$
$\nu_3(0)$		$(0,1)$	$\psi_3(x,y) = \cos(\frac{y}{2})$
$\nu_4(0)$	$\frac{1}{4}$	$(2,0)$	$\psi_4(x,y) = \cos(\frac{x}{2})$

We summarize [12], Propositions (8.5), (8.7), (9.5) and (9.9), into the following theorem.

Theorem 3.1. *With the above notation, the following properties hold.*

1. *For $i \geq 1$, the functions $[0,1] \ni a \mapsto \delta_i(a)$, resp. $[0,1] \ni a \mapsto \nu_i(a)$, are non-increasing.*
2. *For $i \geq 1$, the functions $]0,1[\ni a \mapsto \delta_i(a)$, resp. $]0,1[\ni a \mapsto \nu_i(a)$, are continuous.*
3. *For $i \geq 1$, $\lim_{a\to 0+} \delta_i(a) = \delta_i(0)$ and $\lim_{a\to 0+} \nu_i(a) = \nu_i(0)$.*

It follows that for a positive, small enough, we have

$$\begin{cases} 0 < \delta_1(a) \leq \delta_1(0) < \delta_2(a) \leq \delta_2(0) < \delta_3(a) \leq \delta_3(0)\,, \text{and} \\ 0 = \nu_1(a) = \nu_1(0) < \nu_2(a) \leq \nu_2(0) < \nu_3(a) \leq \nu_4(a) \leq \nu_3(0)\,. \end{cases} \tag{3.4}$$

Observe that for $i = 1$ and 2, $\frac{\partial\phi_i}{\partial y}(x,\pi) = 0$ and $\frac{\partial\psi_i}{\partial y}(x,y) = 0$. It follows that for a small enough, the functions ϕ_1 and ϕ_2 (resp. the functions ψ_1 and ψ_2) are the first two eigenfunctions for $\mathcal{R}_a$ with the Dirichlet (resp. Neumann) boundary condition on $\partial\mathcal{R}$, and the Neumann boundary condition on C_a, with associated eigenvalues $\frac{5}{16}$ and $\frac{1}{2}$ (resp. 0 and $\frac{1}{4}$).

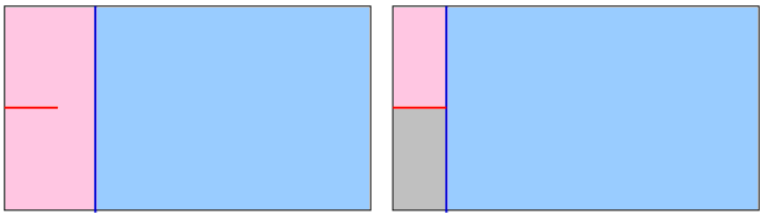

FIGURE 3.1. Rectangle with a crack (Neumann condition)

We have

$$\alpha\phi_1(x,y) + \beta\phi_2(x,y) = \sin(\frac{x}{4})\,\sin(\frac{y}{2})\,\left(\alpha + 2\beta\cos(\frac{x}{4})\right),$$

and

$$\alpha\psi_1(x,y) + \beta\psi_2(x,y) = \alpha + \beta\cos(\frac{x}{4}).$$

We can choose the coefficients α, β in such a way that these linear combinations of the first two eigenfunctions have two (Figure 3.1 left) or three (Figure 3.1 right) nodal domains in $\mathcal{R}_a$.

This proves that the *Extended Courant Property* is false in $\mathcal{R}_a$ with either Dirichlet or Neumann condition on $\partial\mathcal{R}$, and Neumann condition on C_a.

Remark. In the Neumann case, notice that we can introduce several cracks $\{(x, b_j) \mid 0 < x < a_j\}_{j=1}^k$ in such a way that for any $d \in \{2, 3, \dots k+2\}$ there exists a linear combination of 1 and $\cos(\frac{x}{4})$ with d nodal domains.

Remark. Numerical simulations, kindly provided by Virginie Bonnaillie-Noël, indicate that the *Extended Courant Property* does not hold for a rectangle with a crack, with Dirichlet boundary condition on both the boundary of the rectangle, and the crack, see Section 10. Dirichlet cracks appear in another context in [14] (see also references therein).

Remark. It is easy to make an analogous construction for the unit disk (Neumann case) with radial cracks. As computed for example in [16] (Subsection 3.4), the second radial eigenfunction has labelling 6 ($\lambda_6 \approx 14,68$), and we can introduce six radial cracks to obtain a combination of the two first radial Neumann eigenfunctions with seven nodal domains, see Figure 3.2.

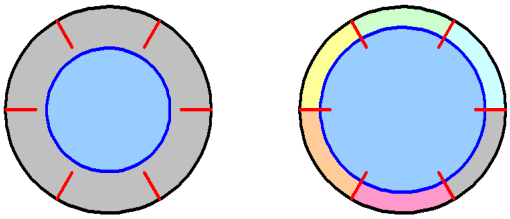

FIGURE 3.2. Disk with cracks, Neumann condition

4. The rectangular flat torus with cracks

Consider the flat torus $\mathbb{T} := \mathbb{R}^2/\left(4\pi\mathbb{Z} \oplus 2\pi Z\right)$. Arrange the eigenvalues in nondecreasing order,

$$\lambda_1(0) < \lambda_2(0) \leq \lambda_3(0) \leq \cdots \tag{4.1}$$

The eigenvalues are given by the numbers $\frac{m^2}{4} + n^2$ for (m, n) pairs of integers, with associated complex eigenfunctions

$$\exp(im\frac{x}{2})\,\exp(iny) \tag{4.2}$$

or equivalently, with real eigenfunctions

$$\begin{aligned} &\cos(m\tfrac{x}{2})\,\cos(ny),\ \cos(m\tfrac{x}{2})\,\sin(ny),\\ &\sin(m\tfrac{x}{2})\,\cos(ny),\ \sin(m\tfrac{x}{2})\,\sin(ny), \end{aligned} \tag{4.3}$$

where m, n are non-negative integers. Accordingly, the first eigenpairs of $\mathcal{T}$ are as follows.

(4.4)

Eigenvalue	Value	Pairs	Eigenfunctions
$\lambda_1(0)$	0	$(0,0)$	$\omega_1(x,y) = 1$
$\lambda_2(0)$			$\omega_2(x,y) = \cos(\frac{x}{2})$
$\lambda_3(0)$	$\frac{1}{4}$	$(1,0)$	$\omega_2(x,y) = \sin(\frac{x}{2})$
$\lambda_4(0)$			$\omega_3(x,y) = \cos(y)$
$\lambda_5(0)$	1	$(0,1)$	$\omega_4(x,y) = \sin(y)$

A typical linear combination of the first three eigenfunctions is of the form $\alpha + \beta\,\sin(\frac{x}{2} - \theta)$

Take the torus $\mathbb{T}$, and perform two (or more) cracks parallel to the x axis, and with the same length a. Call $\mathbb{T}_a$ the torus with cracks, see Figure 4.1, and choose the Neumann boundary condition on the cracks. For a small enough, the first three eigenfunctions of the torus $\mathbb{T}$ remain eigenfunctions of the torus with cracks, $\mathbb{T}_a$, with the same $\tau(\mathbb{T}_a, 3) = 2$. We can choose the length a such that the nodal set of $\alpha + \beta\,\sin(\frac{x}{2} - \theta)$

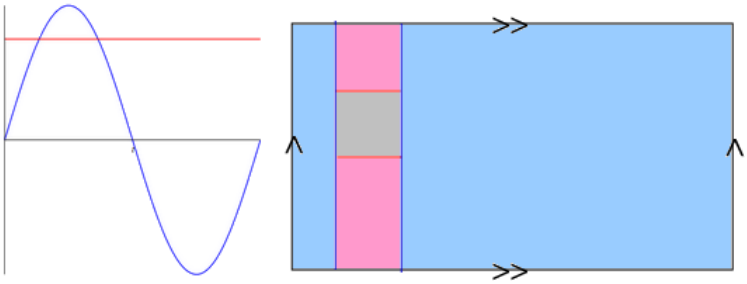

FIGURE 4.1. Flat torus with two cracks

and the two cracks determine three nodal domains. The proof is the same as in [12].

This proves that the *Extended Courant Property* is false on the flat torus with cracks.

5. Sphere $\mathbb{S}^2$ with cracks

On the round sphere $\mathbb{S}^2$, we consider the geodesic lines $z \mapsto (\sqrt{1-z^2}\cos\theta_i, \sqrt{1-z^2}\sin\theta_i, z)$ through the north pole $(0,0,1)$, with distinct $\theta_i \in [0,\pi[$. For example, removing the geodesic segments $\theta_0 = 0$ and $\theta_2 = \frac{\pi}{2}$ with $1 - z \leq a \leq 1$, we obtain a sphere $\mathbb{S}^2_a$ with a crack in the form of a cross. We choose the Neumann boundary condition on the crack.
We can then easily produce a function, in the space generated by the two first eigenspaces of the sphere with a crack, having five nodal domains.

The first eigenvalue of $\mathbb{S}^2$ is $\lambda_1(0) = 0$, with corresponding eigenspace of dimension 1, generated by the function 1. The next eigenvalues of $\mathbb{S}^2$ are $\lambda_2(0) = \lambda_3(0) = \lambda_4(0) = 2$ with associated eigenspace of dimension 3, generated by the functions x, y, z. The following eigenvalues of $\mathbb{S}^2$ are larger than or equal to 6.
As in [12], the eigenvalues of $\mathbb{S}^2_a$ (with Neumann condition on the crack) are non-increasing in a, and continuous to the right at $a = 0$. More precisely

$$\text{(5.1)} \qquad \begin{cases} 0 = \lambda_1(a) < \lambda_2(a) \leq \lambda_3(a) \leq \lambda_4(a) \leq 2 < \lambda_5(a) \leq 6\,, \\ \lim_{a\to 0+} \lambda_i(a) = 2 \text{ for } i = 2,3,4, \\ \lim_{a\to 0+} \lambda_5(a) = 6\,. \end{cases}$$

The function z is also an eigenfunction of $\mathbb{S}^2_a$ with eigenvalue 2. It follows from (5.1) that for a small enough, $\lambda_4(a) = 2$, with eigenfunction z. For $0 < b < a$, the linear combination $z - b$ has five nodal domains in $\mathbb{S}^2_a$, see Figure 5.1 in spherical coordinates.

It follows that the *Extended Courant Property* does not hold on the sphere with cracks.

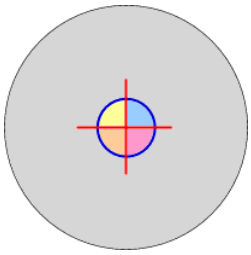

FIGURE 5.1. Sphere with crack, five nodal domains

Remark 1. Removing more geodesic segments around the north pole, we can obtain a linear combination $z - b$ with as many nodal domains as we want.

Remark 2. The sphere with cracks, and Dirichlet condition on the cracks, has been considered for another purpose in [15].

6. The cube with Dirichlet boundary condition

In this section, we adapt the method used in [13] (summarized in Section 2) to the $3D$-case.

Consider the cube $\mathcal{C}_\pi =]0, \pi[^3$. The eigenvalues are the numbers

$$q_3(k, m, n) = k^2 + m^2 + n^2\,, \quad k, m, n \in \mathbb{N}^\bullet.$$

A corresponding complete set of eigenfunctions is given by the functions

$$\phi_{k,m,n}(x, y, z) = \sin(kx)\, \sin(my)\, \sin(nz)\,, \quad k, m, n \in \mathbb{N}^\bullet.$$

The first Dirichlet eigenvalues of the cube are given by

$$\begin{aligned} &\delta_1\ [3] < \delta_2 = \delta_3 = \delta_4\ [6] < \delta_5 = \delta_6 = \delta_7\ [9] < \dots \\ &\quad \delta_8 = \delta_9 = \delta_{10}\ [11] < \delta_{11} \cdots . \end{aligned}$$

Using Chebyshev polynomials, for $k, m, n \in \mathbb{N}^\bullet$ we have

$$\phi_{k,m,n}(x, y, z) = \phi_{1,1,1}(x, y, z)\, U_{k-1}(\cos x)\, U_{m-1}(\cos y)\, U_{n-1}(\cos z)\,.$$

The factor $\phi_{1,1,1}$ does not vanish in the cube $\mathcal{C}_\pi$. The map

$$\mathcal{C}_\pi \ni (x, y, z) \mapsto (X, Y, Z) := (\cos(x), \cos(y), \cos(z)) \in]-1, 1[^3$$

is a diffeomorphism from $\mathcal{C}_\pi$ to the cube $]-1, 1[^3$.

Let $\mathcal{L}_r$ now denote the set $\mathcal{L}(\mathcal{C}_\pi, D, r)$.

In view of the preceding remarks, in order to count the nodal domains of a linear combination $\Phi \in \mathcal{L}_r$,

$$\Phi = \sum_{q_3(k,m,n) \le r} c_{k,m,n}\, \phi_{k,m,n}$$

in the cube $\mathcal{C}_\pi$, it suffices to count the nodal domains of the corresponding linear combination,

$$\Psi = \sum_{q_3(k,m,n)\leq r} c_{k,m,n}\, U_{k-1}(X)U_{m-1}(Y)U_{n-1}(Z)$$

in the cube $]-1,1[^3$.

Using the formulas for the Chebyshev polynomials, it is easy to see that the linear combinations Ψ for $k^2+m^2+n^2 \leq 11 = \delta_{10}$ correspond to the polynomials of degree less than or equal to 2 in the variables X, Y and Z.

In particular, the polynomial $f_a(X,Y,Z) := X^2+Y^2+Z^2-a$ can be represented as such a linear combination Ψ with $k^2+m^2+n^2 \leq 11$. We can consider the corresponding linear combination $\phi_a(x,y,z) \in \mathcal{L}_{11} = \mathcal{L}_{\delta_{10}}$.

When $a<0$, the polynomial f_a is positive in $]-1,1[^3$ and, correspondingly, the function $\phi_a \in \mathcal{L}_{11}$ does not vanish in $\mathcal{C}_\pi$, so that it has one nodal domain.

When $0<a<\sqrt{2}$, the polynomial f_a has two nodal domains in $]-1,1[^3$ and, correspondingly, the function $\phi_a \in \mathcal{L}_{11}$ has two nodal domains in $\mathcal{C}_\pi$.

When $\sqrt{2}<a<\sqrt{3}$, the polynomial f_a has nine nodal domains in $]-1,1[^3$ and, correspondingly, the function $\phi_a \in \mathcal{L}_{11}$ has nine nodal domains in $\mathcal{C}_\pi$.

On the other-hand, $\mathcal{L}_{11}$ involves eigenfunctions associated with eigenvalues less than or equal to 11 i.e., the ten first eigenfunctions. Since $11 = \delta_8 = \delta_9 = \delta_{10}$, Courant's upper bound is $8 = \tau(\mathcal{C}_\pi, D, 10)$.

It follows that ϕ_a, $\sqrt{2}<a<\sqrt{3}$, provides a counterexample to the *Extended Courant Property* for the $3D$-cube with Dirichlet boundary condition.

Remark. The same method can be applied to the cube with Neumann boundary condition, but does apparently not provide counterexamples in this case.

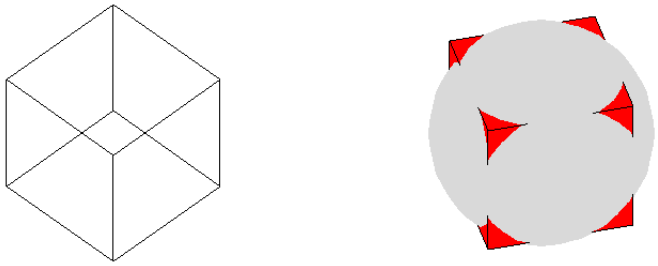

FIGURE 6.1. Cube with Dirichlet boundary condition

7. The equilateral triangle

Let $\mathcal{T}_e$ denote the equilateral triangle with sides equal to 1, see Figure 7.1. The eigenvalues and eigenfunctions of $\mathcal{T}_e$, with either Dirichlet or Neumann condition on the boundary $\partial\mathcal{T}_e$, can be completely described, see [5, 24, 23], or [6]. We provide a summary in Appendix A.

In this section, we show that the equilateral triangle provides a counterexample to the *Extended Courant Property* for both the Dirichlet and the Neumann boundary condition.

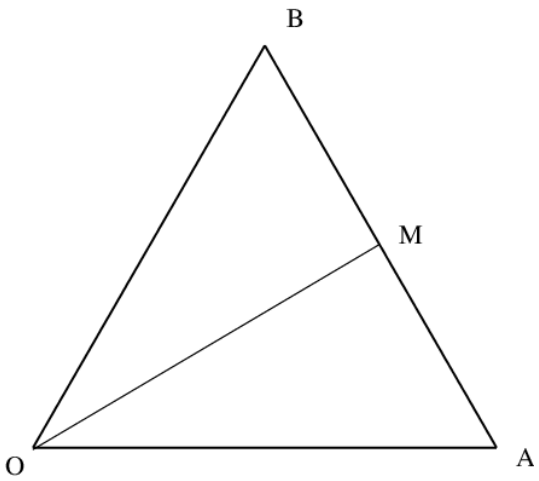

FIGURE 7.1. Equilateral triangle $\mathcal{T}_e = [OAB]$

7.1. **Neumann boundary condition.** The sequence of Neumann eigenvalues of the equilateral triangle $\mathcal{T}_e$ begins as follows,

$$0 = \lambda_1(\mathcal{T}_e, N) < \frac{16\pi^2}{9} = \lambda_2(\mathcal{T}_e, N) = \lambda_3(\mathcal{T}_e, N) < \lambda_4(\mathcal{T}_e, N)\,. \tag{7.1}$$

The second eigenspace has dimension 2, and contains one eigenfunction φ_2^N which is invariant under the mirror symmetry with respect to the median OM, and another eigenfunction φ_3^N which is anti-invariant under the same mirror symmetry, see Appendix A.

More precisely, according to (A.21), the function $\varphi_2^N(x, y)$ can be chosen to be,

$$\left\{ \begin{array}{rl} \varphi_2^N(x,y) = & \cos(\frac{4\pi}{3}x) + \cos(\frac{2\pi}{3}(-x+\sqrt{3}y)) \\ & + \cos(\frac{2\pi}{3}(x+\sqrt{3}y))\,, \end{array} \right. \tag{7.2}$$

or, more simply,

$$\varphi_2^N(x,y) = 2\cos\left(\frac{2\pi x}{3}\right)\left(\cos\left(\frac{2\pi x}{3}\right) + \cos\left(\frac{2\pi y}{\sqrt{3}}\right)\right) - 1\,. \tag{7.3}$$

The set $\{\varphi_2^N + 1 = 0\}$ consists of the two line segments $\{x = \frac{3}{4}\} \cap \mathcal{T}_e$ and $\{x + \sqrt{3}y = \frac{3}{2}\} \cap \mathcal{T}_e$, which meet at the point $(\frac{3}{4}, \frac{\sqrt{3}}{4})$ on $\partial\mathcal{T}_e$.

The sets $\{\varphi_2 + a = 0\}$, with $a \in \{0, 1-\varepsilon, 1, 1+\varepsilon\}$, and small positive ε, are shown in Figure 7.2. When a varies from $1-\varepsilon$ to $1+\varepsilon$, the number of nodal domains of $\varphi_2 + a$ in $\mathcal{T}_e$ jumps from 2 to 3, with the jump occurring for $a = 1$.

It follows that $\varphi_2^N + a = 0$, for $1 \leq a \leq 1.1$, provides a counterexample to the *Extended Courant Property* for the equilateral triangle with Neumann boundary condition.

Figure 7.3 displays the graphs of the function φ_2^N (top left), and of the functions $a + \varphi_2^N$, with $a \in \{0.9, 1, 1.1\}$. The equilateral triangle appears in grey, in the plane $\{z = 0\}$.

Remark. The eigenfunction φ_2^N restricted to the hemiequilateral triangle is the second Neumann eigenfunction of $\mathcal{T}_h = [OAM]$. The restriction of φ_3^N to the hemiequilateral triangle is an eigenfunction of $\mathcal{T}_h$ with mixed boundary condition (Dirichlet on OM and Neumann on the other sides).

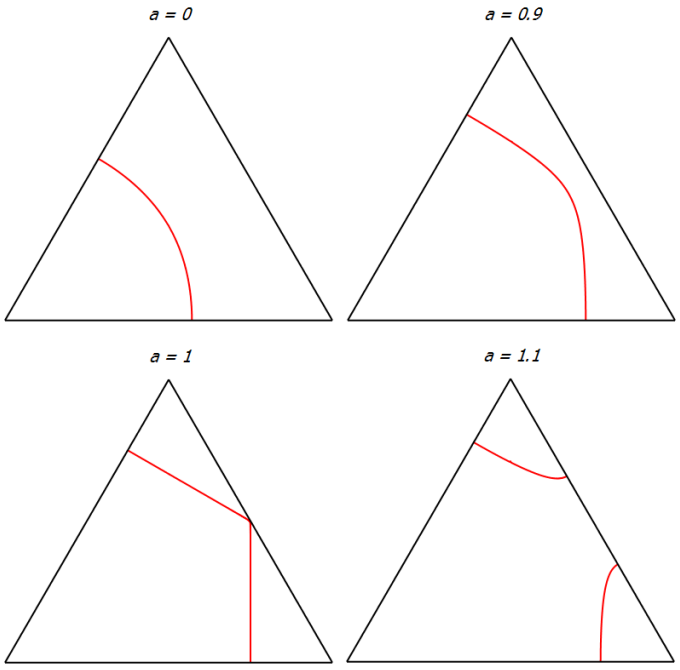

FIGURE 7.2. Levels sets $\{\varphi_2^N + a = 0\}$ for $a \in \{0\,;\,0.9\,;\,1\,;\,1.1\}$

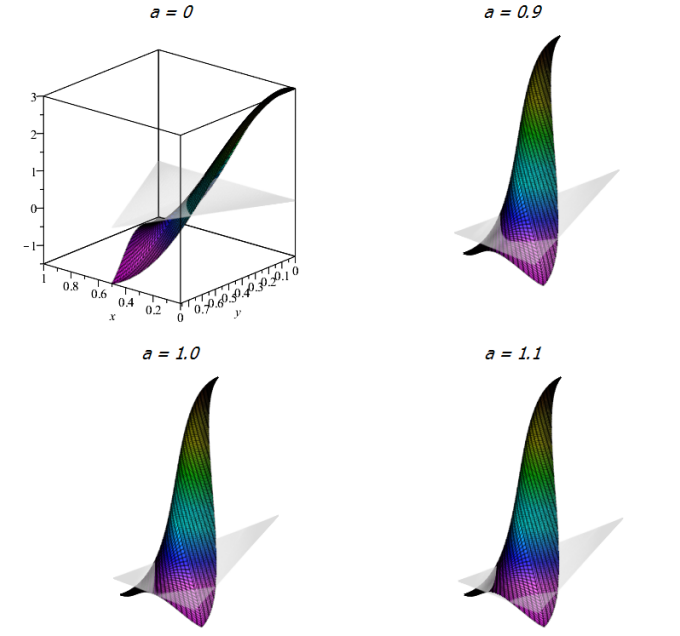

FIGURE 7.3. Counterexample for the Extended Courant Property (Neumann boundary condition)

7.2. **Dirichlet boundary condition.** The sequence of Dirichlet eigenvalues of the equilateral triangle $\mathcal{T}_e$ begins as follows,

$$\delta_1(\mathcal{T}_e) = \frac{16\pi^2}{3} < \delta_2(\mathcal{T}_e) = \delta_3(\mathcal{T}_e) = \frac{112\pi^2}{9} < \delta_4(\mathcal{T}_e). \tag{7.4}$$

More precisely, according to (A.23), the function $\varphi_1^D(x,y)$ can be chosen to be,

$$\begin{aligned} \varphi_1^D(x,y) = \; & 2\sin\left(2\pi(x+\tfrac{y}{\sqrt{3}})\right) - 2\sin\left(4\pi\tfrac{y}{\sqrt{3}}\right) \\ & -2\sin\left(2\pi(x-\tfrac{y}{\sqrt{3}})\right), \end{aligned} \tag{7.5}$$

or, more simply, by

$$\begin{aligned} \varphi_1^D(x,y) &= 4\sin\tfrac{2\pi y}{\sqrt{3}}\left(\cos(2\pi x) - \cos\tfrac{2\pi y}{\sqrt{3}}\right), \\ &= -8\,\sin\tfrac{2\pi y}{\sqrt{3}}\,\sin\pi(x+\tfrac{y}{\sqrt{3}})\,\sin\pi(x-\tfrac{y}{\sqrt{3}}), \end{aligned} \tag{7.6}$$

which shows that φ_1^D does not vanish inside $\mathcal{T}_e$.

The second eigenvalue has multiplicity 2, with one eigenfunction φ_2^D symmetric with respect to the median OM, and the other φ_3^D antisymmetric.

More precisely, according to (A.25), the function φ_2^D can be chosen to be,

$$\begin{aligned} \varphi_2^D(x,y) = \; & \sin\left(\tfrac{2\pi}{3}(5x+\sqrt{3}y)\right) - \sin\left(\tfrac{2\pi}{3}(5x-\sqrt{3}y)\right) \\ & + \sin\left(\tfrac{2\pi}{3}(x-3\sqrt{3}y)\right) - \sin\left(\tfrac{2\pi}{3}(x+3\sqrt{3}y)\right) \\ & + \sin\left(\tfrac{4\pi}{3}(2x+\sqrt{3}y)\right) - \sin\left(\tfrac{4\pi}{3}(2x-\sqrt{3}y)\right). \end{aligned} \tag{7.7}$$

We now consider the linear combination $\varphi_2^D + a\,\varphi_1^D$, with a close to 1. Figure 7.4 is obtained by numerical computations.

Figure 7.5 displays the graphs of the function φ_2^D (top left), and of the functions $\varphi_2^D + a\varphi_1^D$, with $a \in \{0.8, 1, 1.1\}$. The equilateral triangle appears in grey, in the plane $\{z = 0\}$.

Figure 7.4 looks very much like Figure 7.2, and we can suspect that there is a hidden relation between $\varphi_2^D + a\,\varphi_1^D$ and $\varphi_2^N + a$. This is indeed the case, as Lemma 7.1 below shows.

It follows that, when $0 < a < 1$, the function $\varphi_2^D + a\,\varphi_1^D$ has two nodal domains; when $1 \le a < 1.1$, it has three nodal domains.

The function $\varphi_2^D + a\,\varphi_1^D$, for $1 \le a \le 1.1$, provides a counterexample to the *Extended Courant Property* for the equilateral triangle with the Dirichlet boundary condition.

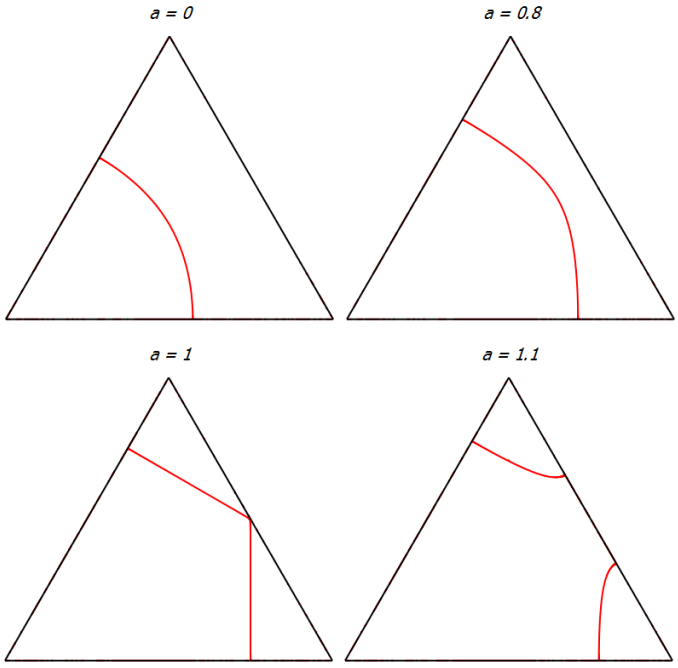

FIGURE 7.4. Levels sets $\{\varphi_2^D + a\,\varphi_1^D = 0\}$ for $a \in \{0\,;\,0.8\,;\,1\,;\,1.1\}$

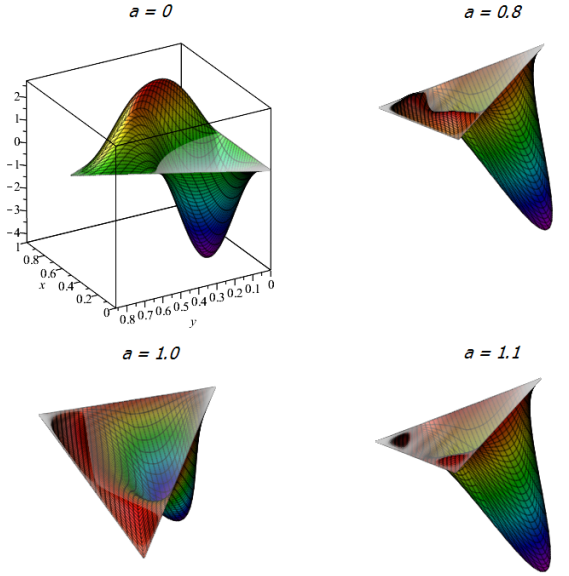

FIGURE 7.5. Counterexample for the Extended Courant Property (Dirichlet boundary condition)

7.3. **Relation between φ_2^D and φ_2^N.**

Lemma 7.1. *With the above notation, the following equality holds,*

$$\varphi_2^D = \varphi_1^D \varphi_2^N \,.$$

Proof. We express the above eigenfunctions in terms of $X := \cos\frac{2\pi}{3}x$ and $Y := \cos\frac{2\pi}{\sqrt{3}}y$.

First we observe from (7.3) that

$$\varphi_2^N(x,y) = 2X(X+Y) - 1\,.$$

Secondly, we have from (7.6)

$$\varphi_1^D(x,y) = 2\sin\frac{2\pi y}{\sqrt{3}}\,(8X^3 - 6X - 2Y)\,.$$

Finally, it remains to compute φ_2^D. We start from (7.7), and first factorize $\sin\frac{2\pi y}{\sqrt{3}}$ in each line. More precisely, we write,

(7.8)

$$\begin{aligned}
&\sin\tfrac{2\pi}{3}(5x+\sqrt{3}y) - \sin\tfrac{2\pi}{3}(5x-\sqrt{3}y) = 2\sin(\tfrac{2\pi y}{\sqrt{3}})\cos(5\tfrac{2\pi x}{3})\,,\\
&\sin\tfrac{2\pi}{3}(x-3\sqrt{3}y) - \sin\tfrac{2\pi}{3}(x+3\sqrt{3}y) = -2\sin(3\tfrac{2\pi y}{\sqrt{3}})\cos(\tfrac{2\pi x}{3})\,,\\
&\sin\tfrac{4\pi}{3}(2x+\sqrt{3}y) - \sin\tfrac{4\pi}{3}(2x-\sqrt{3}y) = 2\sin(2\tfrac{2\pi y}{\sqrt{3}})\cos(4\tfrac{2\pi x}{3})\,.
\end{aligned}$$

We now use the classical Chebyshev polynomials T_n, U_n, and the relations $\cos(n\theta) = T_n(\cos\theta)$ and $\sin(n+1)\theta = \sin(\theta)\,U_n(\cos\theta)$.

This gives,

$$\begin{aligned}
\varphi_2^D &= 2\sin\tfrac{2\pi y}{\sqrt{3}}\Big(T_5(X) - XU_2(Y) + T_4(X)U_1(Y)\Big)\\
&=: 2\sin\tfrac{2\pi y}{\sqrt{3}}\,Q(X,Y)\,.
\end{aligned}$$

We find that

$$Q(X,Y) = 16X^5 - 20X^3 + 6X + 2Y(8X^4 - 8X^2 + 1) - 4XY^2\,,$$

and it turns out that the polynomial $Q(X,Y)$ can be factorized as

$$Q(X,Y) = \Big(2X(X+Y) - 1\Big)\,(8X^3 - 6X - 2Y)\,,$$

so that $\varphi_2^D = \varphi_1^D\varphi_2^N$.

In the above computation, we have used the relations,

$$T_4(X) = 8X^4 - 8X^2 + 1\,,\; T_5(X) = 16X^5 - 20X^3 + 5X\,,$$

and

$$U_1(Y) = 2Y\,,\; U_2(Y) = 4Y^2 - 1\,.$$

□

8. The regular hexagon

We are looking for another counterexample for the Extended Courant Property in a convex domain of $\mathbb{R}^2$. We have already mentioned that this quest was unsuccessful for the square, see Section 2. It is natural to think of other polygons and, among them, the regular hexagon $\mathcal{H}$.

Call $\mathcal{H} = [ABCDEF]$ the regular hexagon with sides of length 1, $\mathcal{T}_e = [OAB]$ the equilateral triangle, and $\mathcal{T}_h = [OAM]$ the hemiequilateral triangle. See Figure 8.1.

In this section, we consider both the Dirichlet, and the Neumann boundary conditions on $\partial\mathcal{H}$.

8.1. **Preliminaries.** Only a small portion (asymptotically one-sixth) of the eigenvalues, and of the eigenfunctions, of the regular hexagon $\mathcal{H}$ are known explicitly, namely those which arise from the equilateral triangle, or from the hemiequilateral triangle (with Dirichlet or Neumann boundary condition).

Numerical computations of the Dirichlet eigenvalues, and of the nodal patterns of Dirichlet eigenfunctions, are available in the literature, see for example [4, 11]. They strongly rely on the symmetries of the hexagon.

We did not find similar computations for the Neumann eigenvalues and eigenfunctions of $\mathcal{H}$ in the literature. We performed numerical computations for this case with MATLAB, making use of the symmetries as in [11].

Assuming that the computed eigenvalues are close enough to the true eigenvalues, using symmetries and Courant's nodal domain theorem, it is possible to identify the first six Dirichlet or Neumann eigenfunctions of $\mathcal{H}$, and their nodal patterns.

As a consequence, we obtain numerical evidence that the regular hexagon provides counterexamples for the *Extended Courant Property*, for either Dirichlet or Neumann boundary condition.

8.2. **Symmetries.** Figure 8.2 displays the lines of mirror symmetry of the regular hexagon.

For simplicity, we use the same notation for a line, and for the mirror symmetry across that line.

Given $\sigma, \tau \in \{+, -\}$, we consider the following sets of functions,

$$\mathcal{S}_{\sigma,\tau} := \{\varphi \mid \varphi \circ D_1 = \sigma\,\varphi,\ \varphi \circ M_2 = \tau\,\varphi\}\,. \tag{8.1}$$

Because the mirror symmetries with respect to D_1 and M_2 commute, the eigenfunctions of the hexagon can be decomposed according to the

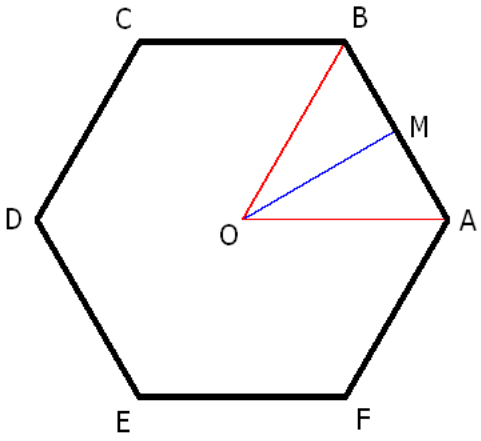

FIGURE 8.1. The hexagon

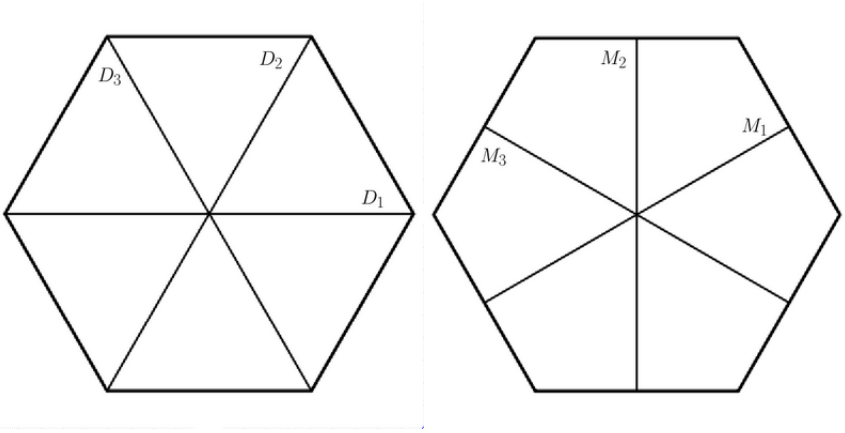

FIGURE 8.2. The lines of symmetry of the hexagon

four sets $\mathcal{S}_{\sigma,\tau}$. Eigenfunctions in one of these sets correspond to eigenfunctions of the domain $\mathcal{R}$, see Figure 8.3, with mixed boundary conditions. For example, the Dirichlet eigenfunctions of $\mathcal{H}$ which belong to $\mathcal{S}_{+,-}$, correspond to eigenfunctions of the domain $\mathcal{R}$ with Dirichlet condition on the line $[ABQ]$, Neumann condition on the side $[OA]$, and Dirichlet condition on the side $[OQ]$. Similar descriptions can be made for the other cases.

We also introduce the subsets,

$$\mathcal{S}_{\sigma,\tau} \supseteq \mathcal{S}^0_{\sigma,\tau} := \{\varphi \mid \varphi \circ D_i = \sigma\,\varphi,\ \varphi \circ M_j = \tau\,\varphi,\ \ 1 \leq i,j \leq 3\}\,. \tag{8.2}$$

The eigenfunctions of $\mathcal{H}$ in one of these subsets arise from eigenfunctions of the hemiequilateral triangle $\mathcal{T}_h$, with mixed boundary conditions.

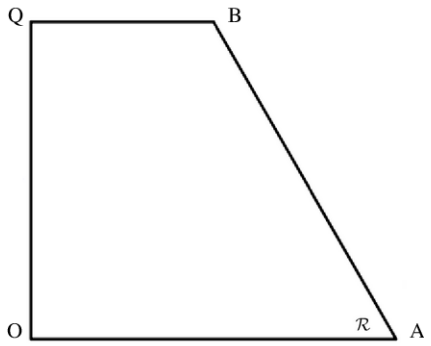

FIGURE 8.3. The domain $\mathcal{R}$

The Dirichlet and Neumann eigenvalues of $\mathcal{T}_e$ and $\mathcal{T}_h$ can be described explicitly, together with complete sets of eigenfunctions, see [5, 24, 23], or [6] and Appendix A for a summary. The eigenvalues and eigenfunctions of $\mathcal{T}_h$ with mixed boundary conditions are, generally speaking, not known explicitly.

For example, the first Dirichlet eigenfunction $u_{1,D}$ of $\mathcal{H}$ arises from the first eigenfunction for $\mathcal{T}_h$, with mixed boundary condition NND (sides listed in decreasing order of length), i.e., Dirichlet condition on the smaller side, Neumann on the other sides of $\mathcal{T}_h$.

Note that the eigenfunctions of $\mathcal{H}$ which belong to $\mathcal{S}^0_{+,-}$ or to $\mathcal{S}^0_{-,+}$ have at least 6 nodal domains. According to Courant's nodal domain theorem, they correspond to eigenvalues with index at least 6. Similarly, the eigenfunctions of $\mathcal{H}$ which belong to $\mathcal{S}^0_{-,-}$ have at least 12 nodal domains, and hence correspond to eigenvalues with index at least 12.

Letting R denote the rotation with center the origin, and angle $\frac{2\pi}{3}$, define the map

$$T(\varphi) = \varphi \circ R - \varphi \circ R^2 \,. \tag{8.3}$$

One can show that T maps $\mathcal{S}_{\sigma,\tau}$ into $\mathcal{S}_{-\sigma,-\tau}$, with kernel $\mathcal{S}^0_{\sigma,\tau}$, and that it is a bijection from the orthogonal of $\mathcal{S}^0_{\sigma,\tau}$ in $\mathcal{S}_{\sigma,\tau}$ onto the orthogonal of $\mathcal{S}^0_{-\sigma,-\tau}$ in $\mathcal{S}_{-\sigma,-\tau}$ (orthogonality with respect to the $L^2(\mathcal{H})$ inner product).

8.3. **Numerical computations.** Fix a boundary condition B on $\partial\mathcal{H}$, either Dirichlet or Neumann. Numerically compute the eigenvalues of $\mathcal{R}$, with the boundary condition B on $\partial\mathcal{R}\cap\partial\mathcal{H}$, and with mixed boundary conditions on the other sides. Merge the four sets of numerical eigenvalues, and re-order the result to obtain the numerical eigenvalues of $\mathcal{H}$, with boundary condition B. In order to identify eigenfunctions in $\mathcal{S}^0_{\sigma,\tau}$, compute the eigenvalues of $\mathcal{T}_h$, with boundary condition B on $\partial\mathcal{T}_h \cap \partial\mathcal{H}$, and with mixed boundary conditions on the other sides.

It turns out that the low lying eigenvalues of $\mathcal{R}$ and $\mathcal{T}_h$ are simple. It follows that one can identify the low lying eigenvalues of $\mathcal{H}$ corresponding to eigenfunctions in the classes $\mathcal{S}_{\sigma,\tau}$ and $\mathcal{S}^0_{\sigma,\tau}$, for $\sigma, \tau \in \{+, -\}$. Using the map T, one can identify the double eigenvalues of $\mathcal{H}$.

8.4. **Dirichlet boundary condition.** Figure 8.4, reproduced from [4], displays the nodal patterns of the twenty-one first Dirichlet eigenfunctions of $\mathcal{H}$. We produced Figure 8.5 with MATLAB.

The computations indicate that the 6-th eigenvalue is simple, and that the nodal set of the corresponding Dirichlet eigenfunction $u_{6,D}$ is a closed simple line. Taking for granted that $\delta_6(\mathcal{H})$ is simple, using the symmetries of the hexagon, and making use of Courant's nodal domain theorem, one can show that $u_{6,D}$ actually belongs to $\mathcal{S}^0_{+,+}$. It follows that it arises from the second eigenfunction of $\mathcal{T}_h$, with mixed boundary condition NND (Dirichlet on the smaller side, Neumann on the other sides).

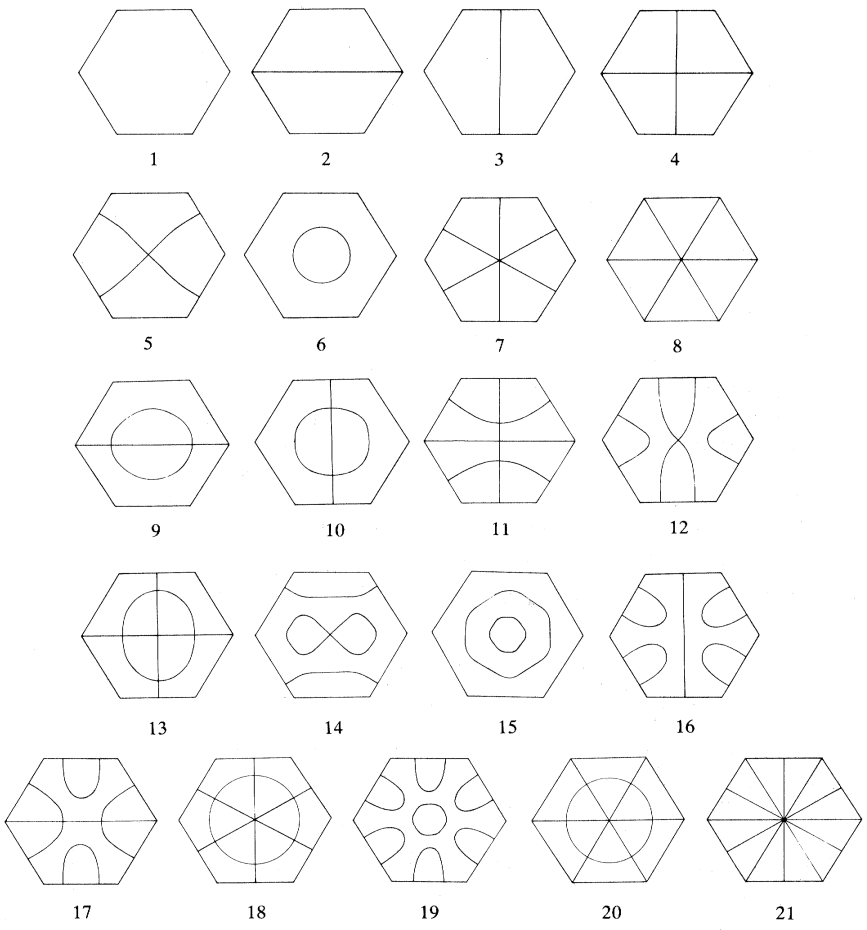

FIGURE 8.4. Nodal structure for the Dirichlet Laplacian in the hexagon [4, Fig. 2]

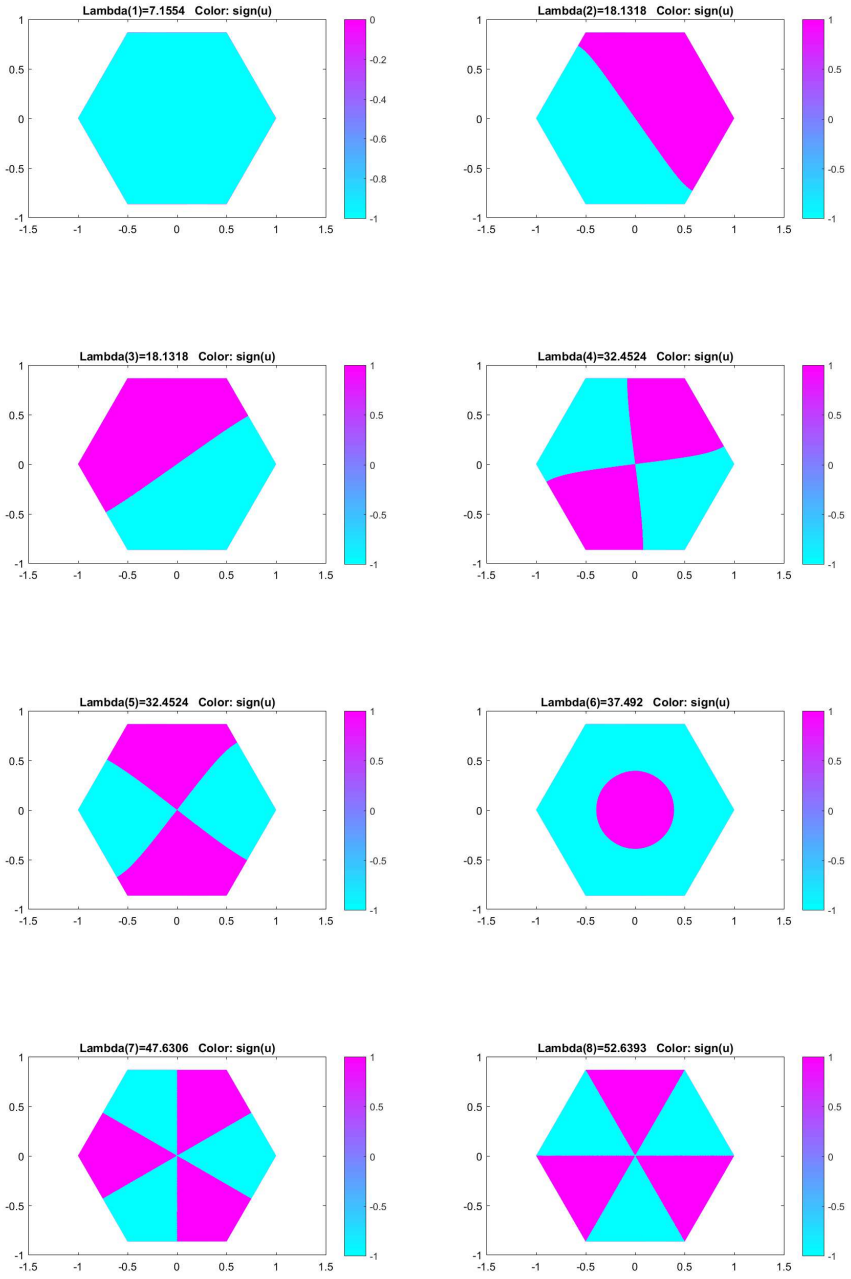

FIGURE 8.5. Eigenpairs for the hexagon with Dirichlet condition using MATLAB

The corresponding nodal patterns in Figure 8.4 and Figure 8.5 appear as slightly different. This is because we have 2-dimensional eigenspaces

associated with $\lambda_2 = \lambda_3$ and $\lambda_4 = \lambda_5$. The computations in [4] (Figure 8.4) take the symmetries into account from the beginning. Figure 8.5 was produced with MATLAB, directly on the hexagon, the computed eigenfunctions are not always the symmetric ones. This figure is provided for comparison with the Neumann case below, see Figure 8.6.

Concerning the Extended Courant Property, the natural question is:

Question 1: Does there exist a linear combination of $u_{1,D}$ and $u_{6,D}$ with at least 7 nodal domains?

Consider $\mathcal{T}_h$ with mixed boundary condition NND. Call f_1 a first eigenfunction, and f_2 a second eigenfunction. To answer Question 1, it suffices to prove that a level line of f_2/f_1 cuts the equilateral triangle into three parts.

As far as we know, the eigenfunctions f_2 and f_1 are not known trigonometric polynomials. This is stated in [25, Section 3], without proof.

This question can at least be tackled numerically (the main difficulty being that both f_1 and f_2 vanish on one side).

Numerical simulations, kindly provided by Virginie Bonnaillie-Noël, suggest that the answer to Question 1 is positive. See Section 10.

8.5. **Neumann boundary condition.** The first eigenpairs for the hexagon $\mathcal{H}$ with Neumann boundary condition, as computed with MATLAB, are shown in Figure 8.6.

The first Neumann eigenfunction of the hexagon is 0, with associated eigenfunction $u_{1,N} \equiv 1$. Figure 8.6 suggests that the 6-th Neumann eigenvalue of the hexagon has multiplicity 2, and that the nodal set of one of the associated eigenfunction is a simple closed curve. The figure also suggests that the corresponding eigenfunction $u_{6,N}$ is invariant under all mirror symmetries of the hexagon, and hence that it is obtained from an eigenfunction of the hemiequilateral triangle $\mathcal{T}_h$ with Neumann boundary condition. The computed value ≈ 17.5474 shows that this corresponds to the second Neumann eigenfunction of the hemiequilateral triangle, associated with the eigenvalue $\frac{16\pi^2}{9}$.

Figure 8.7 displays the results of two MATLAB computations for $\nu_6(\mathcal{H})$ and $\nu_7(\mathcal{H})$, with different mesh sizes. They indicate that it is not always easy to identify the eigenfunctions via numerical computations when the eigenvalue is degenerate (although, in this case, one still sees the rotational symmetry with angle $\frac{2\pi}{3}$). This difficulty can be avoided by using symmetries from the start, and computing the eigenvalues of the domain $\mathcal{R}$ as explained above.

As far as the Extended Courant Property is concerned, the natural question is:

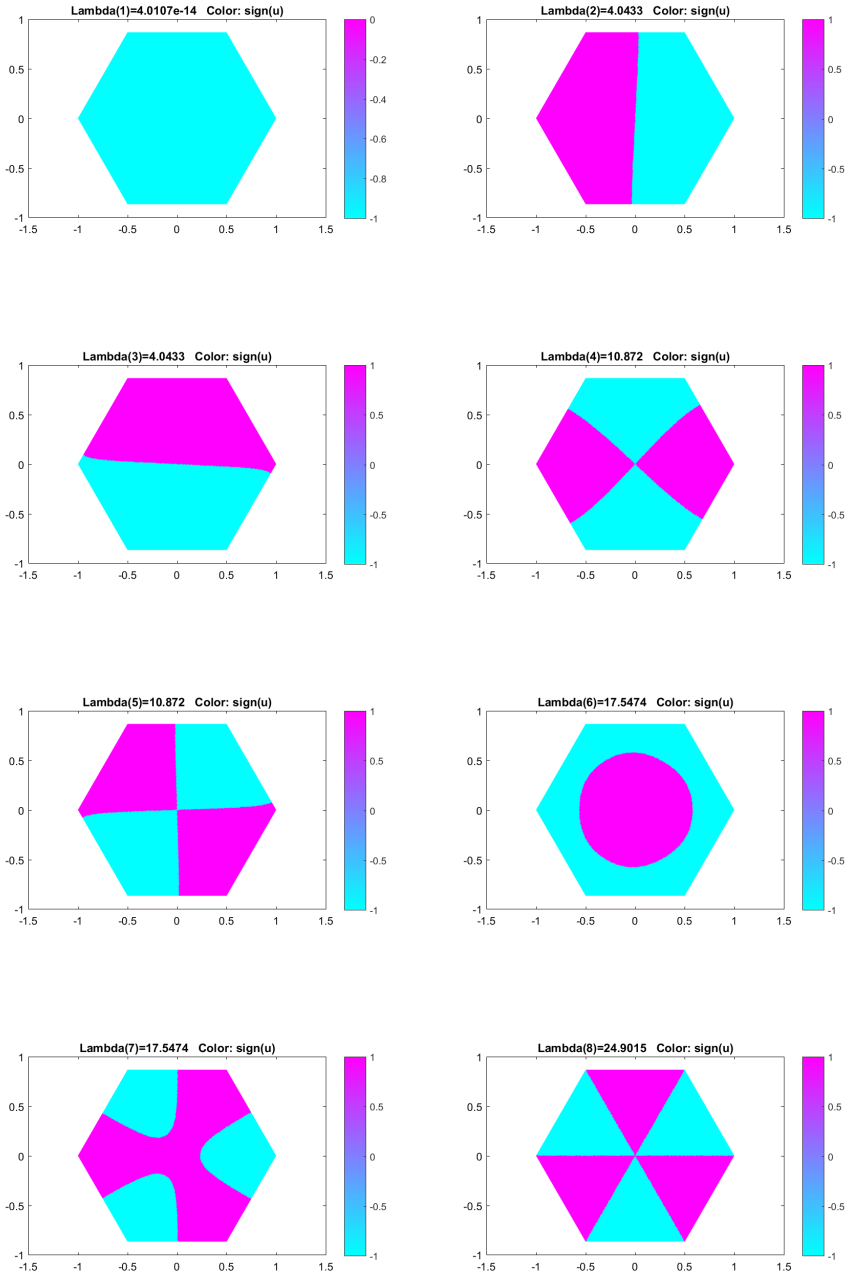

FIGURE 8.6. Eigenpairs for the hexagon with Neumann condition using MATLAB

Question 2: Does there exist a linear combination of $u_{1,N}$ and $u_{6,N}$ with at least 7 nodal domains?

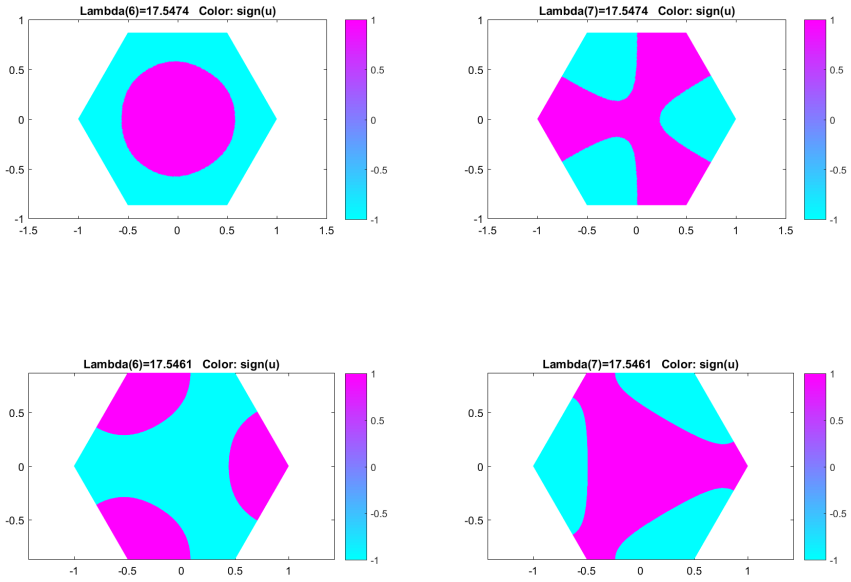

FIGURE 8.7. Two MATLAB computations for $\nu_6(\mathcal{H})$ and $\nu_7(\mathcal{H})$

In order to identify the eigenspace E associated with the Neumann eigenvalue $\nu_6(\mathcal{H})$, we use the numerical computations of the eigenvalues of the domain $\mathcal{R}$, with the Neumann boundary condition on the line $[ABQ]$, and either Dirichlet or Neumann boundary condition on the sides $[OA]$ and $[OQ]$. Assume that the numerically computed eigenvalues are close enough to the true eigenvalues. Using the numerical or exact computations of the eigenvalues arising from the triangle $\mathcal{T}_h$, possibly with mixed boundary conditions, symmetries and Courant's theorem, one can infer that E contains an eigenfunction $u_{6,N}$ arising from the second eigenvalue of $\mathcal{T}_h$ with Neumann boundary condition, and an eigenfunction $u_{7,N}$ arising from the first eigenvalue of $\mathcal{T}_h$ with mixed boundary condition NDN (with sides ordered by decreasing length). Both eigenvalues are explicitly known, and are eigenvalues of the equilateral triangle.

The function $u_{6,N} + a$ of the hexagon $\mathcal{H}$ is obtained from the function $\varphi_2^N + a$ of the equilateral triangle $\mathcal{T}_e$, by reflections with respect to the diagonals of the hexagon. Using Subsection 7.1, see Figure 7.2, we see that when a varies from 0 to $1 + \varepsilon$ the number of nodal domains of $u_{6,N} + a$ in $\mathcal{H}$ jumps from 2 to 7, with the jump occurring for $a = 1$.

It follows that the *Extended Courant property* does not hold on the regular hexagon with Neumann boundary condition.

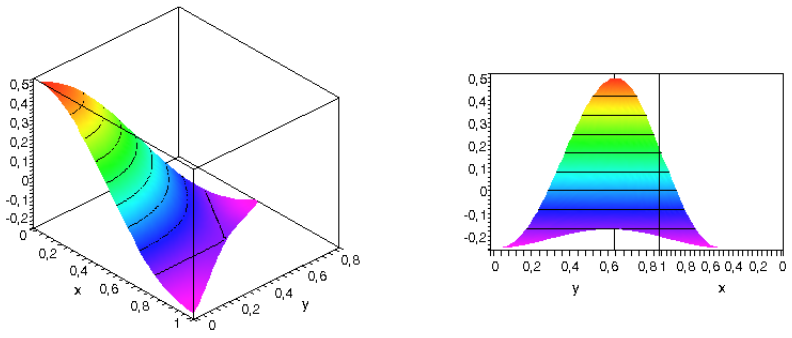

FIGURE 8.8. Equilateral triangle: 2nd Neumann eigenfunction (symmetric one)

9. Extensions

In the case of a Euclidean domain $\Omega \subset \mathbb{R}^d$, with the Dirichlet boundary condition, another natural upper bound for the number of nodal domains is provided by Pleijel's method [26] which uses the Faber-Krahn isoperimetric inequality. Namely, for $u \in \lambda_n(\Omega, D)$ we have

$$\beta_0(u) \leq |\Omega| \left(\frac{\lambda_n(\Omega, D)}{\lambda_1(\mathbb{B}_1^d, D)} \right)^{\frac{d}{2}} , \tag{9.1}$$

where $|\Omega|$ is the Euclidean volume of Ω, and where $\mathbb{B}_1^d$ is the Euclidean ball with volume 1. When n tend to infinity the right-hand side of (9.1) is asymptotically smaller than or equal to $\gamma(d)\, n$ for some positive constant $\gamma(d) < 1$.

It would be natural to investigate the *Extended Courant Property* with Courant's bound replaced by Pleijel's bound (9.1).

10. Further numerical simulations

The numerical simulations in this section were kindly performed by Virginie Bonnaillie-Noël. The eigenvalues and eigenfunctions are computed using a finite element method [22]. Similar simulations are done in [8] to determine the minimal 3-partition of a square.

Rectangle with a crack, and Dirichlet boundary condition. Figure 10.1 shows (from top to bottom) the level lines of v_1, v_2, the first and second eigenfunctions of the rectangle with a horizontal crack, with Dirichlet boundary condition on both the crack and the boundary of the rectangle. In this example, the length of the rectangle is equal to twice the width. The crack begins on the left side, at half the width; its length is equal to $\frac{1}{10}$ of the length of the rectangle.

The third picture shows the level lines of the quotient $\frac{v_2}{v_1}$, and suggests that the linear combination $2v_1 - v_2$ has three nodal domains, two of them on each side of the crack.

One can therefore **conjecture that the *Extended Courant Property* does not hold on a rectangle with a crack and Dirichlet boundary condition.**

Hexagon with Dirichlet boundary condition. Figure 10.2 shows (from top to bottom) the level lines of f_1, f_2, the first and second eigenfunctions of the equilateral triangle, with Dirichlet boundary condition on one side, Neumann condition on the other sides. Here, f_1 and f_2 are normalized by the conditions $\sup_{\mathcal{T}} f_1 = 1$ and $\sup_{\mathcal{T}} f_2 = 1$.

The third picture shows the level lines of the quotient $\frac{f_2}{f_1}$, and suggests that the linear combination $\frac{3}{2}f_1 + f_2$ has three nodal domains, two of them in the neighborhood of the vertices of the side with Dirichlet boundary condition.

The first and sixth Dirichlet eigenfunctions of the hexagon are obtained from the functions f_1 and f_2 by reflection with respect to the diagonals of the hexagon. Figure 10.3 shows (from top to bottom) the level lines of $u_{1,D}$, $u_{6,D}$, the first and sixth eigenfunctions of the hexagon with Dirichlet boundary condition. The third picture shows the level lines of the quotient $\frac{u_{6,D}}{u_{1,D}}$.

The pictures suggest that $\frac{3}{2}u_{1,D} + u_{2,D}$ has seven nodal domains, six near the vertices of the hexagon and one containing the center O.

One can therefore **conjecture that the *Courant Extended Property* does not hold on the regular hexagon with Dirichlet boundary condition.**

Regular polygons. Figure 10.4 shows the nodal lines of the ratio $\frac{w_{6,D}}{w_{1,D}}$ where $w_{1,D}$ (resp. $w_{6,D}$) is the first (resp. sixth) eigenfunction of a regular polygon with 7 sides and Dirichlet boundary condition.

One can therefore **conjecture that the *Extended Courant Property* does not hold for the regular heptagon**. When n tends to infinity, the eigenvalues of the regular polygon with n sides tend to the eigenvalues of the disk. Observing that the second radial eigenfunction of the Dirichlet or Neumann problem for the disk have labelling 6.

One may **more generally conjecture that the *Extended Courant Property* does not hold for the regular polygon with $n \geq 6$ sides, and Dirichlet or Neumann boundary condition.**

This method does not seem to yield a counterexample for the regular pentagon.

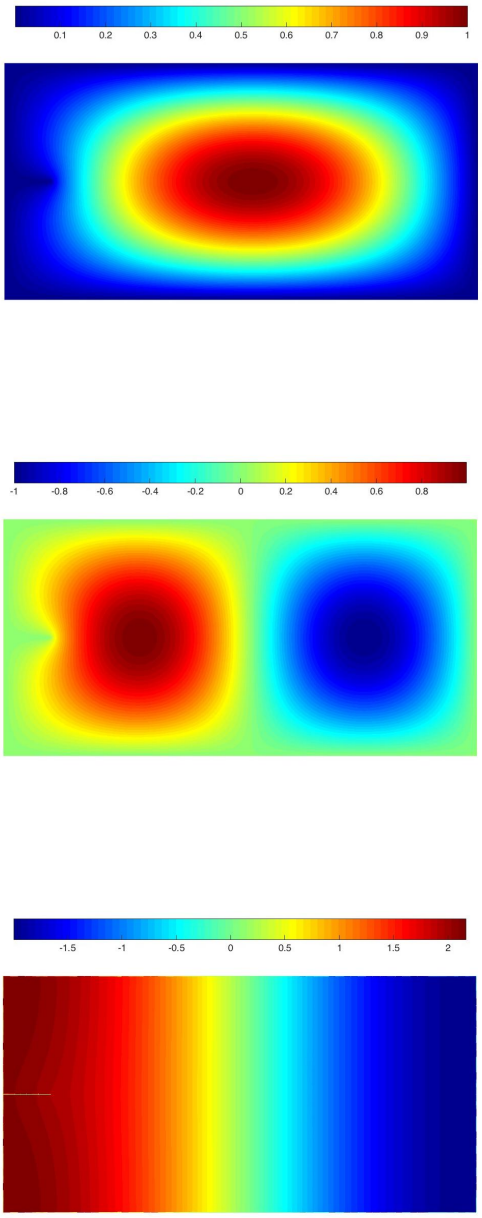

FIGURE 10.1. Level lines of v_1, v_2 and $\frac{v_2}{v_1}$ in a rectangle with an horizontal crack coming from the left

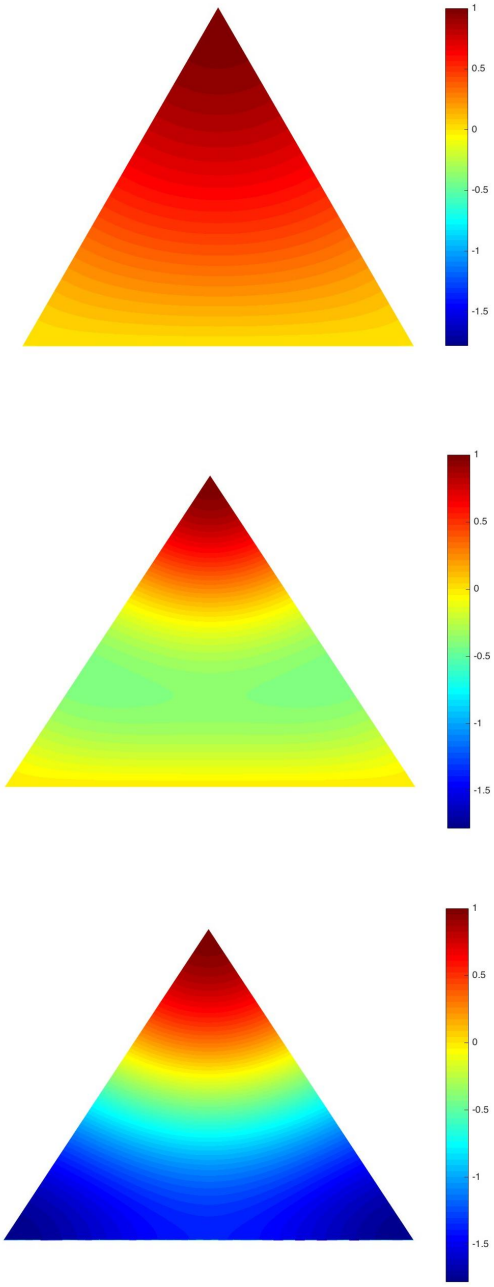

FIGURE 10.2. Level lines of f_1, f_2 and $\frac{f_2}{f_1}$ for the NND problem in the equilateral triangle

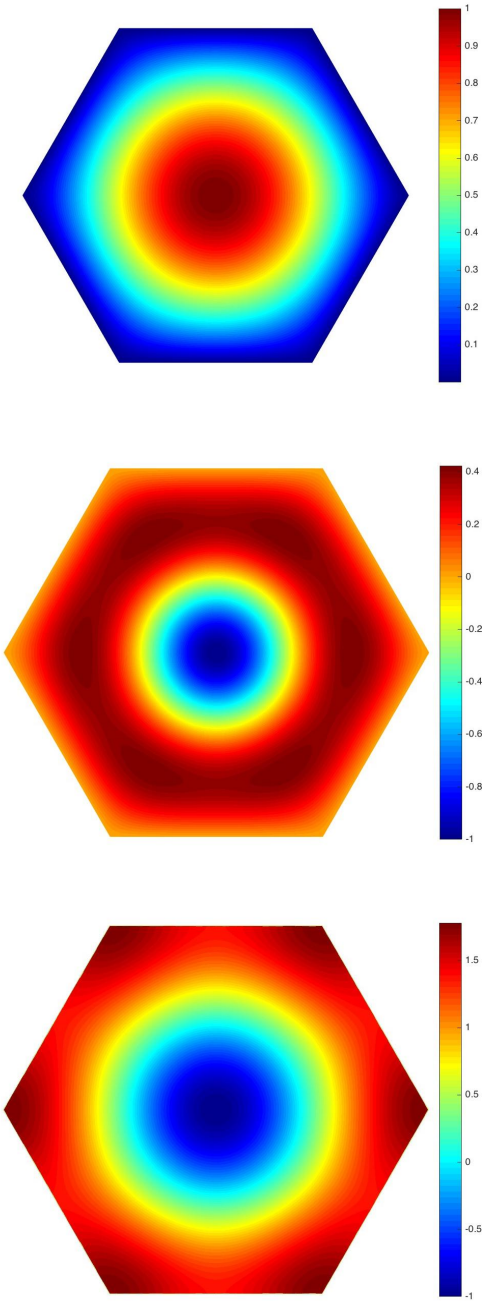

FIGURE 10.3. Level lines of $u_{1,D}, u_{6,D}$ and $\frac{u_{6,D}}{u_{1,D}}$ for the Dirichlet problem in the regular hexagon

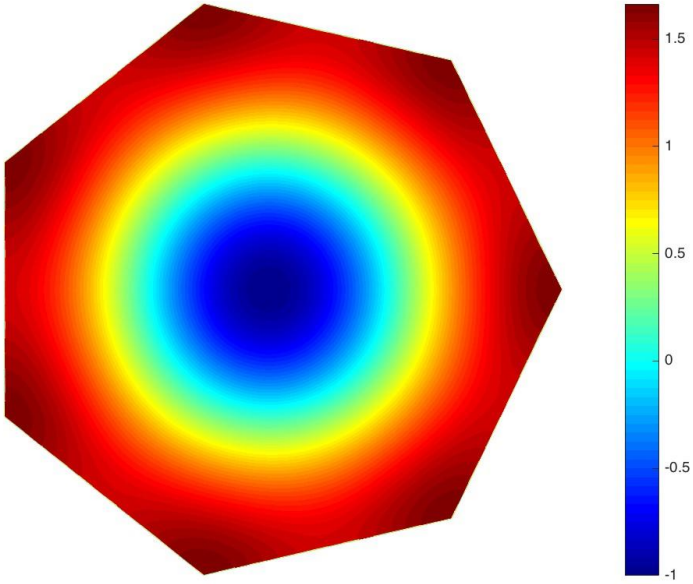

FIGURE 10.4. Level lines of $\frac{w_{6,D}}{w_{1,D}}$ for the Dirichlet problem in the regular heptagon

Appendix A. Eigenvalues of the equilateral triangle

In this appendix, we recall the description of the eigenvalues of the equilateral triangle. For the reader's convenience, we retain the notation of [6, Section 2].

A.1. **General formulas.** Let $\mathbb{E}^2$ be the Euclidean plane with the canonical orthonormal basis $\{e_1 = (1,0), e_2 = (0,1)\}$, scalar product $\langle \cdot, \cdot \rangle$ and associated norm $|\cdot|$.

Consider the vectors

$$\alpha_1 = (1, -\frac{1}{\sqrt{3}}), \alpha_2 = (0, \frac{2}{\sqrt{3}}), \alpha_3 = (1, \frac{1}{\sqrt{3}}) = \alpha_1 + \alpha_2\,, \tag{A.1}$$

and

$$\alpha_1^\vee = (\frac{3}{2}, -\frac{\sqrt{3}}{2}), \alpha_2^\vee = (0, \sqrt{3}), \alpha_3^\vee = (\frac{3}{2}, \frac{\sqrt{3}}{2}) = \alpha_1^\vee + \alpha_2^\vee\,. \tag{A.2}$$

Then

$$\alpha_i^\vee = \frac{3}{2}\alpha_i, |\alpha_i|^2 = \frac{4}{3}, |\alpha_i^\vee|^2 = 3. \tag{A.3}$$

Define the mirror symmetries

$$s_i(x) = x - 2\frac{\langle x, \alpha_i\rangle}{\langle \alpha_i, \alpha_i\rangle}\alpha_i = x - \frac{2}{3}\langle x, \alpha_i^\vee\rangle \alpha_i^\vee\,, \tag{A.4}$$

whose axes are the lines

$$L_i = \{x \in \mathbb{E}^2 \mid \langle x, \alpha_i\rangle = 0\}. \tag{A.5}$$

Let W be the group generated by these mirror symmetries. Then,

$$W = \{1, s_1, s_2, s_3, s_1 \circ s_2, s_1 \circ s_1\}\,, \tag{A.6}$$

where $s_1 \circ s_2$ (resp. $s_2 \circ s_1$) is the rotation with center the origin and angle $\frac{2\pi}{3}$ (resp. $-\frac{2\pi}{3}$).

Remark. The above vectors are related to the root system A_2 and W is the Weyl group of this root system.

Let

$$\Gamma = \mathbb{Z}\alpha_1^\vee \oplus \mathbb{Z}\alpha_2^\vee \tag{A.7}$$

be the (equilateral) lattice. The set

$$\mathcal{D}_\Gamma = \{s\alpha_1^\vee + t\alpha_2^\vee \mid 0 \le s, t \le 1\} \tag{A.8}$$

is a fundamental domain for the action of Γ on $\mathbb{E}^2$. Another fundamental domain is the closure of the open hexagon (see Figure 8.1)

$$\mathcal{H} = [A, B, C, D, E, F]\,, \tag{A.9}$$

whose vertices are given by

$$\begin{cases} A = (1,0); B = (\frac{1}{2}, \frac{\sqrt{3}}{2}); (-\frac{1}{2}, \frac{\sqrt{3}}{2}); \\ D = (-1,0); E = (-\frac{1}{2}, -\frac{\sqrt{3}}{2}); F = (\frac{1}{2}, -\frac{\sqrt{3}}{2})\,. \end{cases} \tag{A.10}$$

Call $\mathcal{T}_e$ the equilateral triangle

$$\mathcal{T}_e = [O, A, B]\,, \tag{A.11}$$

where $O = (0, 0)$.
Let Γ^* be the dual lattice of the lattice Γ, defined by

$$\Gamma^* = \{x \in \mathbb{E}^2 \mid \forall \gamma \in \Gamma, \langle x, \gamma\rangle \in \mathbb{Z}\}\,. \tag{A.12}$$

Then,

$$\begin{cases} \Gamma^* = \mathbb{Z}\varpi_1 \oplus \mathbb{Z}\varpi_2\,, \\ \text{where } \varpi_1 = (\frac{2}{3}, 0) \text{ and } \varpi_2 = (\frac{1}{3}, \frac{1}{\sqrt{3}})\,. \end{cases} \tag{A.13}$$

Define the set C (an open Weyl chamber of the root system A_2),

$$C = \{x\varpi_1 + y\varpi_2 \mid x, y > 0\}\,, \tag{A.14}$$

and let $\mathbb{T}_e$ denote the equilateral torus $\mathbb{E}^2/\Gamma$.

A complete set of orthogonal (not normalized) eigenfunctions of $-\Delta$ on $\mathbb{T}_e$ is given (in complex form) by the exponentials

$$\phi_p(x) = \exp(2i\pi\langle x, p\rangle) \text{ where } x \in \mathbb{E}^2 \text{ and } p \in \Gamma^*\,. \tag{A.15}$$

Furthermore, for $p = m\varpi_1 + n\varpi_2$, with $m, n \in \mathbb{Z}$, the multiplicity of the eigenvalue $\hat{\lambda}(m, n) = 4\pi^2|p|^2 = \frac{16\pi^2}{9}(m^2 + mn + n^2)$ is equal to the number of points (k, ℓ) in $\mathbb{Z}^2$ such that $k^2 + k\ell + \ell^2 = m^2 + mn + n^2$.

The closure of the equilateral triangle $\mathcal{T}_e$ is a fundamental domain of the action of the semi-direct product $\Gamma \rtimes W$ on $\mathbb{E}^2$ or equivalently, a fundamental domain of the action of W on $\mathbb{T}_e^2$.

For the following proposition, we refer to [5].

Proposition A.1. *Complete orthogonal (not normalized) sets of eigenfunctions of the equilateral triangle $\mathcal{T}_e$ in complex form are given, respectively for the Dirichlet (resp. Neumann) boundary condition on $\partial\mathcal{T}_e$, as follows.*

(1) *Dirichlet boundary condition on $\partial\mathcal{T}_e$. The family is*

$$\Phi_p^D(x) = \sum_{w\in W} det(w) exp(2i\pi\langle x, w(p)\rangle) \tag{A.16}$$

with $p \in C \cap \Gamma^*$. Furthermore, for $p = m\varpi_1 + n\varpi_2$, with m, n positive integers, the multiplicity of the eigenvalue $4\pi^2|p|^2$ is equal to the number of solutions $q \in C \cap \Gamma^*$ of the equation $|q|^2 = |p|^2$.

(2) *Neumann boundary condition on $\partial\mathcal{T}_e$. The family is*

$$\Phi_p^N(x) = \sum_{w\in W} exp(2i\pi\langle x, w(p)\rangle) \tag{A.17}$$

with $p \in \overline{C} \cap \Gamma^*$. Furthermore, for $p = m\varpi_1 + n\varpi_2$, with m, n non-negative integers, the multiplicity of the eigenvalue $4\pi^2|p|^2$

is equal to the number of solutions $q \in \overline{C} \cap \Gamma^*$ *of the equation* $|q|^2 = |p|^2$.

Remark. To obtain corresponding complete orthogonal sets of real eigenfunctions, it suffices to consider the functions

$$C_p = \Re(\Phi_p) \text{ and } S_p = \Im(\Phi_p)\,.$$

For $p = m\varpi_1 + n\varpi_2$, with $m, n \in \mathbb{N} \setminus \{0\}$ for the Dirichlet boundary condition (resp. $m, n \in \mathbb{N}$ for the Neumann boundary condition), we denote these functions by $C_{m,n}$ and $S_{m,n}$.

In order to give explicit formulas for the first eigenfunctions, we have to examine the action of the group W on the lattice Γ^*. A simple calculation yields the following table in which we simply denote $m\varpi_1 + n\varpi_2$ by (m, n).

(A.18)

w	(m,n)	$w(m,n)$	$\det(w)$
1	(m,n)	(m,n)	1
s_1	(m,n)	$(-m, m+n)$	-1
s_2	(m,n)	$(m+n, -n)$	-1
s_3	(m,n)	$(-n, -m)$	-1
$s_1 \circ s_2$	(m,n)	$(-m-n, m)$	1
$s_2 \circ s_1$	(m,n)	$(n, -m-n)$	1

Remark. The above table should be compared with [6, Table], in which there is a slight unimportant error (the lines $s_1 \circ s_2$ and $s_2 \circ s_1$ are interchanged).

Remark. Using the above chart, one can easily prove the following relations.

(A.19)
$$\begin{cases} C^D_{n,m} = -C^D_{m,n} & \text{and} \quad S^D_{n,m} = S^D_{m,n}\,, \\ C^N_{n,m} = C^N_{m,n} & \text{and} \quad S^N_{n,m} = -S^N_{m,n}\,. \end{cases}$$

A.2. **Neumann boundary condition, first three eigenfunctions.** The first Neumann eigenvalue of $\mathcal{T}_e$ is 0, corresponding to the point $0 = (0,0) \in \Gamma^*$, with first eigenfunction $\varphi_1 \equiv 1$ up to scaling.

The second Neumann eigenvalue corresponds to the pairs $(1,0)$ and $(0,1)$. According to the preceding remark, it suffices to consider $C^N_{1,0}$

and $S^N_{1,0}$. Using Proposition A.1, and the table (A.18), we find that, at the point $[s,t] = s\alpha_1^\vee + t\alpha_2^\vee$,

$$\text{(A.20)} \qquad \begin{cases} C^N_{1,0}([s,t]) = 2\left(\cos(2\pi s) + \cos(2\pi(-s+t)) + \cos(2\pi t)\right), \\ S^N_{1,0}([s,t]) = 2\left(\sin(2\pi s) + \sin(2\pi(-s+t)) - \sin(2\pi t)\right). \end{cases}$$

Up to a factor 2, this gives the following two independent eigenfunctions for the Neumann eigenvalue $\frac{16\pi^2}{9}$, in the (x,y) variables, with $(x,y) = \left(\frac{3}{2}s, -\frac{\sqrt{3}}{2}s + \sqrt{3}t\right)$ or $(s,t) = \left(\frac{2}{3}x, \frac{1}{3}x + \frac{1}{\sqrt{3}}y\right)$,

$$\text{(A.21)} \qquad \begin{cases} \varphi^N_2(x,y) = & \cos(\frac{4\pi}{3}x) + \cos(\frac{2\pi}{3}(-x+\sqrt{3}y)) \\ & + \cos(\frac{2\pi}{3}(x+\sqrt{3}y)), \\ \varphi^N_3(x,y) = & \sin(\frac{4\pi}{3}x) + \sin(\frac{2\pi}{3}(-x+\sqrt{3}y)) \\ & - \sin(\frac{2\pi}{3}(x+\sqrt{3}y)). \end{cases}$$

The first eigenfunction is invariant under the mirror symmetry with respect to the median OM of the equilateral triangle, see Figure 7.1. The second eigenfunction is anti-invariant under the mirror symmetry with respect to this median. Its nodal set is equal to the median itself.

A.3. **Dirichlet boundary condition, first three eigenfunctions.** The first Dirichlet eigenvalue of $\mathcal{T}_e$ is $\delta_1(\mathcal{T}_e) = \frac{16\pi^2}{3}$. A first eigenfunction is given by $S^D_{1,1}$. Using Proposition A.1, and Table A.18, we find that this eigenfunction is given, at the point $[(s,t] = s\alpha_1^\vee + t\alpha_2^\vee$, by the formula

$$\text{(A.22)} \qquad \begin{cases} \varphi^D_1([s,t]) = & 2\sin 2\pi(s+t) + 2\sin 2\pi(s-2t) \\ & + 2\sin 2\pi(t-2s). \end{cases}$$

Substituting the expressions of s and t in terms of x and y, one obtains the formula,

$$\text{(A.23)} \qquad \begin{aligned} \varphi^D_1(x,y) = \; & 2\sin\left(2\pi(x+\tfrac{y}{\sqrt{3}})\right) - 2\sin\left(4\pi\tfrac{y}{\sqrt{3}}\right) \\ & -2\sin\left(2\pi(x-\tfrac{y}{\sqrt{3}})\right), \end{aligned}$$

The second Dirichlet eigenvalue has multiplicity 2, $\delta_2(\mathcal{T}_e) = \delta_3(\mathcal{T}_e) = \frac{112\pi^2}{9}$. The eigenfunctions $C^D_{2,1}$ and $S^D_{2,1}$ are respectively anti-invariant and invariant under the mirror symmetry with respect to $[OM]$, with values at the point $[(s,t)]$ given by the formulas,

$$\text{(A.24)} \qquad \begin{cases} \varphi^D_2([s,t]) = & \sin 2\pi(2s+t) + \sin 2\pi(s+2t) \\ & + \sin 2\pi(2s-3t) - \sin 2\pi(3s-2t) \\ & + \sin 2\pi(s-3t) - \sin 2\pi(3s-t), \\ \varphi^D_3([s,t]) = & \cos 2\pi(2s+t) - \cos 2\pi(s+2t) \\ & - \cos 2\pi(2s-3t) + \cos 2\pi(3s-2t) \\ & + \cos 2\pi(s-3t) - \cos 2\pi(3s-t). \end{cases}$$

Substituting the expressions of s and t in terms of x and y, one obtains the formulas,

$$\begin{aligned}\varphi_2^D(x,y) = \;& \sin\left(\tfrac{2\pi}{3}(5x+\sqrt{3}y)\right) - \sin\left(\tfrac{2\pi}{3}(5x-\sqrt{3}y)\right) \\ & + \sin\left(\tfrac{2\pi}{3}(x-3\sqrt{3}y)\right) - \sin\left(\tfrac{2\pi}{3}(x+3\sqrt{3}y)\right) \\ & + \sin\left(\tfrac{4\pi}{3}(2x+\sqrt{3}y)\right) - \sin\left(\tfrac{4\pi}{3}(2x-\sqrt{3}y)\right)\,.\end{aligned} \tag{A.25}$$

and

$$\begin{aligned}\varphi_3^D(x,y) = \;& \cos\left(\tfrac{2\pi}{3}(5x+\sqrt{3}y)\right) - \cos\left(\tfrac{2\pi}{3}(5x-\sqrt{3}y)\right) \\ & + \cos\left(\tfrac{2\pi}{3}(x-3\sqrt{3}y)\right) - \cos\left(\tfrac{2\pi}{3}(x+3\sqrt{3}y)\right) \\ & + \cos\left(\tfrac{4\pi}{3}(2x+\sqrt{3}y)\right) - \cos\left(\tfrac{4\pi}{3}(2x-\sqrt{3}y)\right)\,.\end{aligned} \tag{A.26}$$

References

[1] V. Arnold. The topology of real algebraic curves (the works of Petrovskii and their development). Uspekhi Math. Nauk. 28:5 (1973), 260–262. 3, 38

[2] V. Arnold. Topological properties of eigenoscillations in mathematical physics. Proc. Steklov Inst. Math. 273 (2011), 25–34. 3

[3] Vladimir I. Arnold. Topology of real algebraic curves (Works of I.G. Petrovskii and their development). Translated by Oleg Viro (from [1]). in Collected works, Volume II. Hydrodynamics, Bifurcation theory and Algebraic geometry, 1965–1972. Edited by A.B. Givental, B.A. Khesin, A.N. Varchenko, V.A. Vassilev, O.Ya. Viro. Springer 2014. http://dx.doi.org/10.1007/978-3-642-31031-7 . Chapter 27, pages 251–254. http://dx.doi.org/10.1007/978-3-642-31031-7_27 . 3

[4] L. Bauer and E.L. Reiss. Cutoff Wavenumbers and Modes of Hexagonal Waveguides. SIAM Journal on Applied Mathematics, 35:3 (1978), 508–514. 19, 22, 24

[5] P. Bérard. Spectres et groupes cristallographiques. Inventiones Math. 58 (1980), 179–199. 13, 21, 34

[6] P. Bérard and B. Helffer. Courant-sharp eigenvalues for the equilateral torus, and for the equilateral triangle. Letters in Math. Physics 106 (2016). 13, 21, 33, 35

[7] P. Bérard and B. Helffer. Sturm's theorem on zeros of linear combinations of eigenfunctions. arXiv:1706.08247. 2

[8] V. Bonnaillie-Noël, B. Helffer and G. Vial. Numerical simulations for nodal domains and spectral minimal partitions. ESAIM: Control, Optimisation and Calculus of Variations 16:1 (2010), 221–246. 27

[9] R. Courant and D. Hilbert. Methoden der mathematischen Physik. Erster Band. Zweite verbesserte Auflage. Julius Springer 1931. 2

[10] R. Courant and D. Hilbert. Methods of mathematical physics. Vol. 1. First English edition. Interscience, New York 1953. 2, 3

[11] L.M. Cureton and J.R. Kuttler. Eigenvalues of the Laplacian on regular polygons and polygons resulting from their disection. Journal of Sound and Vibration 220:1 (1999), 83–98. 19

[12] M. Dauge and B. Helffer. Eigenvalues variation II. Multidimensional problems. J. Diff. Eq. 104 (1993), 263–297. 6, 7, 10

[13] G. Gladwell and H. Zhu. The Courant-Herrmann conjecture. ZAMM - Z. Angew. Math. Mech. 83:4 (2003), 275–281. 3, 4, 6, 11

[14] B. Helffer and T. Hoffmann-Ostenhof and S. Terracini. Nodal domains and spectral minimal partitions. Ann. Inst. H. Poincaré Anal. Non Linéaire 26 (2009), 101–138. 8

[15] B. Helffer and T. Hoffmann-Ostenhof and S. Terracini On spectral minimal partitions: the case of the sphere. In *Around the Research of Vladimir Maz'ya III*. International Math. Series, Springer, Vol. 13, p. 153–178 (2010). 11

[16] B. Helffer and M. Persson-Sundqvist. On nodal domains in Euclidean balls. ArXiv:1506.04033v2. Proc. Amer. Math. Soc. 144 (2016), no. 11, 4777–4791. 8

[17] H. Herrmann. Beiträge zur Theorie der Eigenwerte und Eigenfunktionen. Göttinger Dissertation defended May 20, 1931. Teubner 1932. 2

[18] H. Herrmann. Beziehungen zwischen den Eigenwerten und Eigenfunktionen verschiedener Eigenwertprobleme. Math. Z. 40:1 (1936), 221–241. 3

[19] N. Kuznetsov. On delusive nodal sets of free oscillations. *Newsletter of the European Mathematical Society*, **96** (2015). 3

[20] J. Leydold. On the number of nodal domains of spherical harmonics. PHD, Vienna University (1992). 3

[21] J. Leydold. On the number of nodal domains of spherical harmonics. Topology 35 (1996), 301–321. 3
[22] D. Martin. MÉLINA, bibliothèque de calculs éléments finis (2007). https://anum-maths.univ-rennes1.fr/melina/ . 27
[23] J.B. McCartin. Eigenstructure of the Equilateral Triangle, Part I: The Dirichlet Problem. SIAM Review, 45:2 (2003), 267–287. 13, 21
[24] J.B. McCartin. Eigenstructure of the Equilateral Triangle, Part II: The Neumann Problem. Mathematical Problems in Engineering 8:6 (2002), 517–539. 13, 21
[25] J.B. McCartin. On Polygonal Domains with Trigonometric Eigenfunctions of the Laplacian under Dirichlet or Neumann Boundary Conditions. Applied Mathematical Sciences, Vol. 2, 2008, no. 58, 2891 - 2901. 24
[26] Å. Pleijel. Remarks on Courant's nodal theorem. *Comm. Pure. Appl. Math.* **9** (1956), 543–550. 2, 27
[27] C. Sturm. [No title]. L'institut. Journal général des sociétés et travaux scientifiques de la France et de l'étranger. 1 (1833), 247–248. 2
[28] C. Sturm. Mémoire sur une classe d'équations à différences partielles. Journal de Mathématiques Pures et Appliquées **1** (1836), 373–444. 2
[29] O. Viro. Construction of multi-component real algebraic surfaces. Soviet Math. dokl. 20:5 (1979), 991–995.

PB: INSTITUT FOURIER, UNIVERSITÉ GRENOBLE ALPES AND CNRS, B.P.74, F38402 SAINT MARTIN D'HÈRES CEDEX, FRANCE.
E-mail address: pierrehberard@gmail.com

BH: LABORATOIRE JEAN LERAY, UNIVERSITÉ DE NANTES AND CNRS, F44322 NANTES CEDEX, FRANCE.
E-mail address: Bernard.Helffer@univ-nantes.fr